Cosmic rays muon flux studies at Belgrade shallow underground laboratory

Nikola Veselinović, Mihailo Savić, Aleksandar Dragić, Dimitrije Maletić, Dejan Joković, Radomir Banjanac, Vladimir Udovičić and David Knežević

Inaugural workshop “Cosmic Ray Flux Measurement at Global Scale and the Associated Applications”, Friday, 4 October 2019, Atlanta

Overview

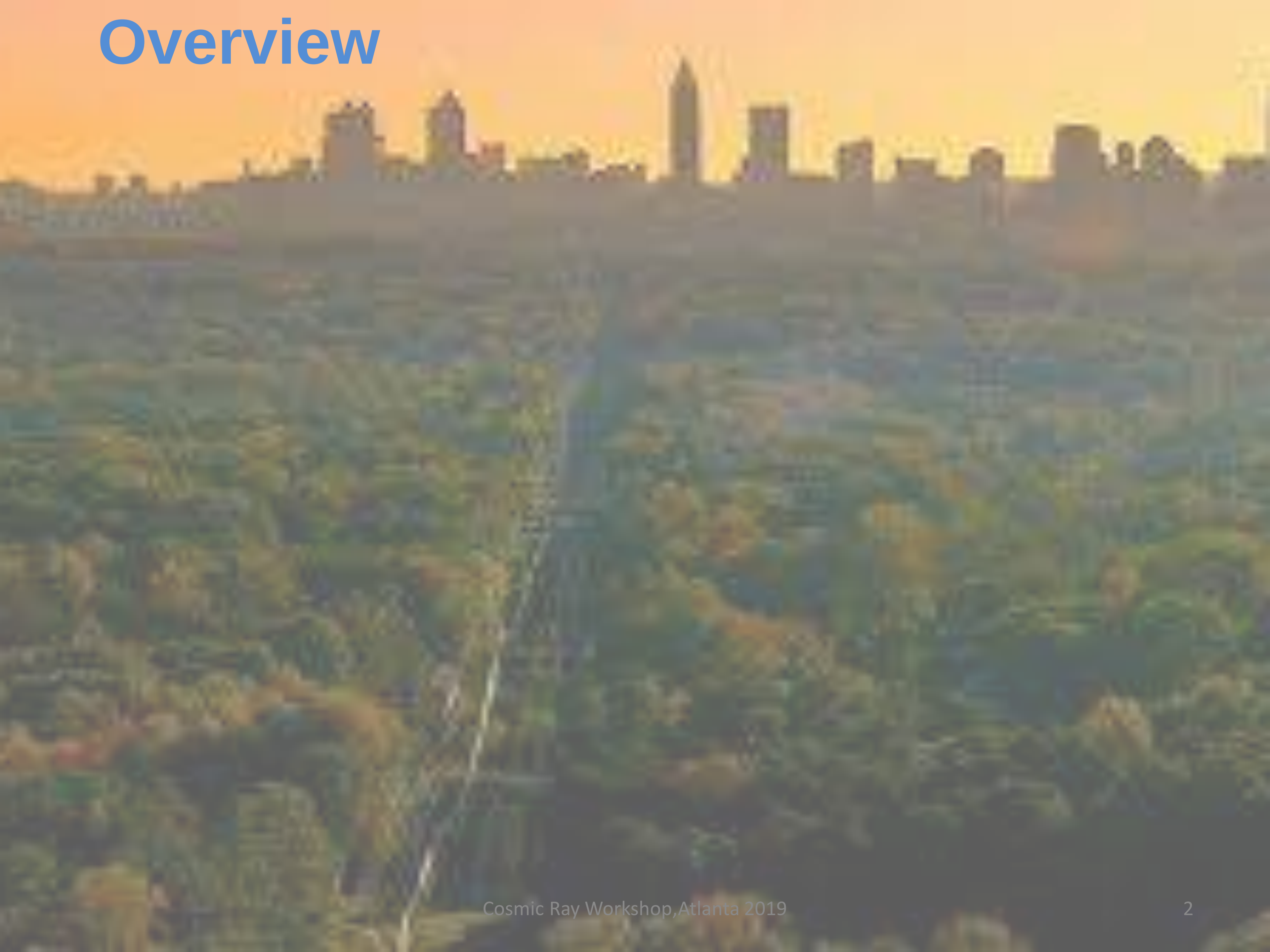

Overview

- Cosmic rays
- Transport through heliosphere
- Transport through geomagnetic field
- Interaction with atmosphere
- Detection of cosmic rays

Overview

- Cosmic rays
- Transport through heliosphere
- Transport through geomagnetic field
- Interaction with atmosphere
- Detection of cosmic rays
- The Belgrade group
- Low-background laboratory
- Past activities
- Cosmic rays physics at Low-background lab
- Measurement of solar activity
  - Comparison between ground detectors
  - Comparison with satellite
- Muons and temperature of the atmosphere
- Cloudiness and CR
- Small arduino detector
- Plans for future
- Conclusion

Cosmic rays

- Major phenomenon in our galaxy
  - Energy density ~ star light, thermal, B field
  - Regulate the equilibrium between the different phases of the interstellar medium
  - Control ionisation, heating
  - Regulate star formation
  - Control astrochemistry
  - Generate turbulent magnetic field
  - Produce Li, Be and B

  Major unknown
  - Sources are not well known (Galactic and Extragal.)
  - Acceleration processes are uncertain

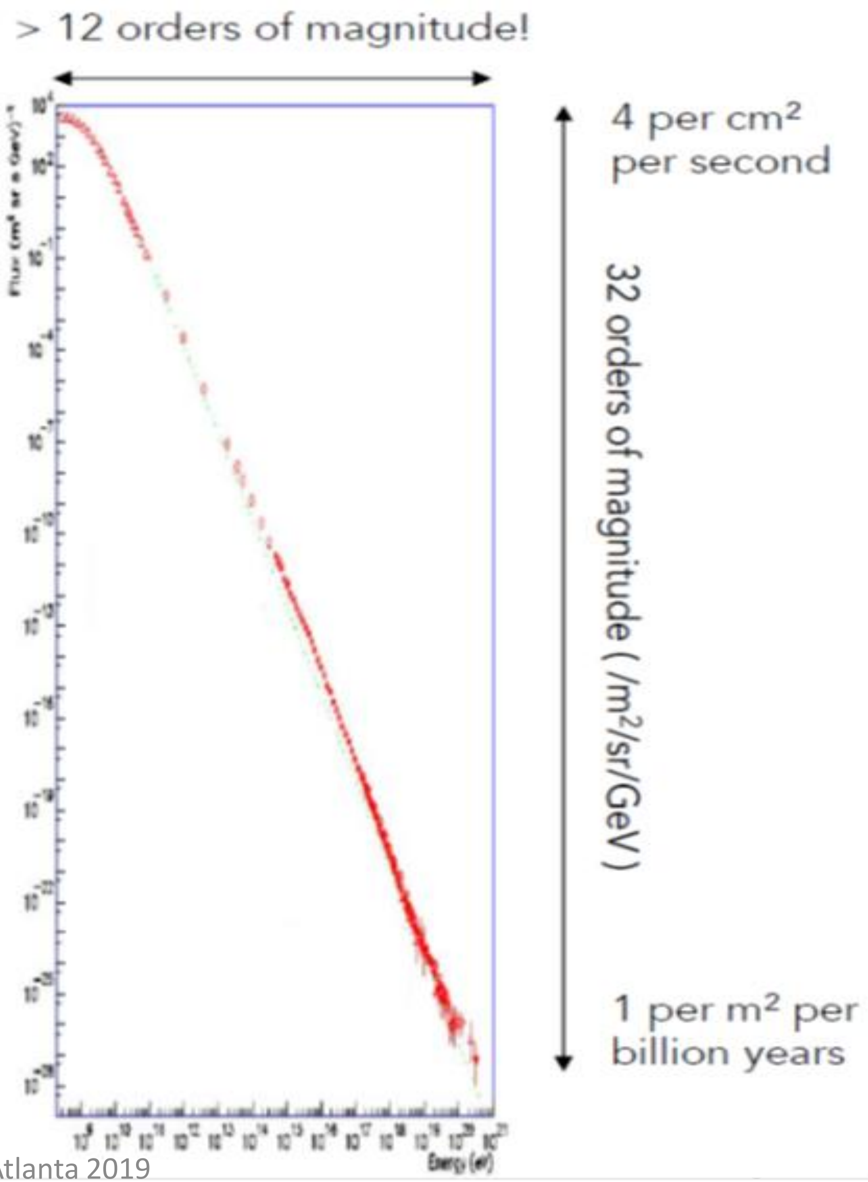

Cosmic rays

- Primary cosmic rays spectrum
  - Power law

$$j(E) = \frac{dN}{dE} \propto E^{-\gamma}$$

- $\gamma \sim 2.7$
- Cosmic rays composition
  - Depends on CR energy
  - ~80% protons, ~12% helium nuclei rest are electrons and nuclei of hevier elements

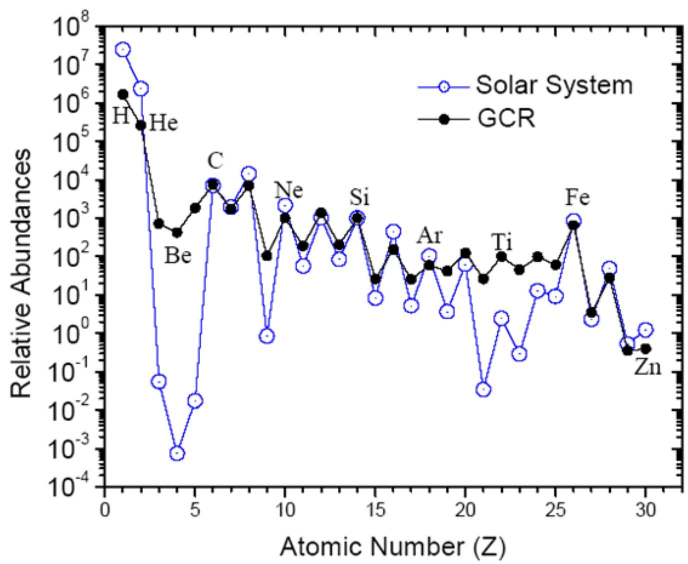

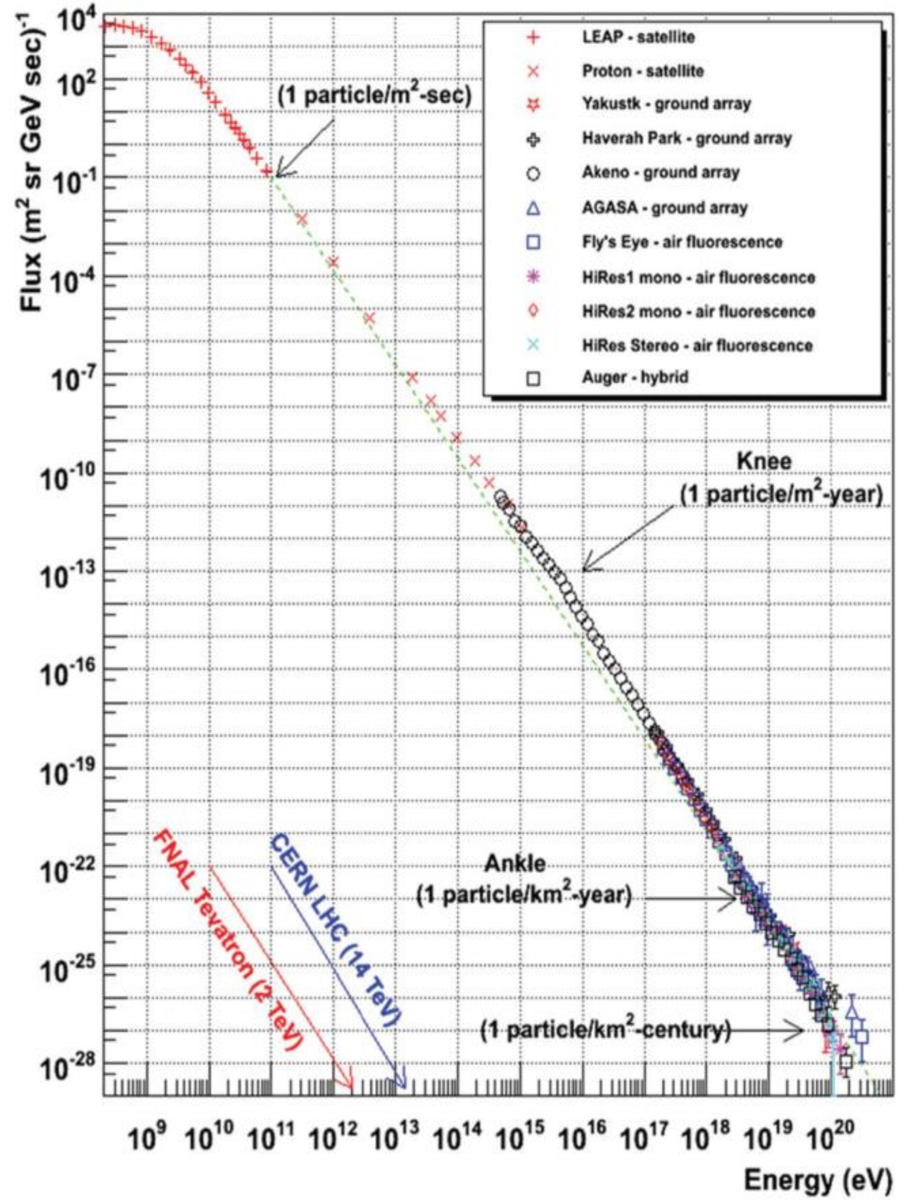

Transport through heliosphere

- **Solar wind**
  - stream of charged particles released from the upper atmosphere of the Sun
- CR interact with helioshere - **modulation of CR**
- Magnetic field and solar wind depend on activity of the Sun (**space weather**)
- CR modulation increases with higher solar and decreases when activity is lower.
- Solar modulation depends on energy of the CR
- **Magnetic rigidity**

$R \equiv pc / Ze$.

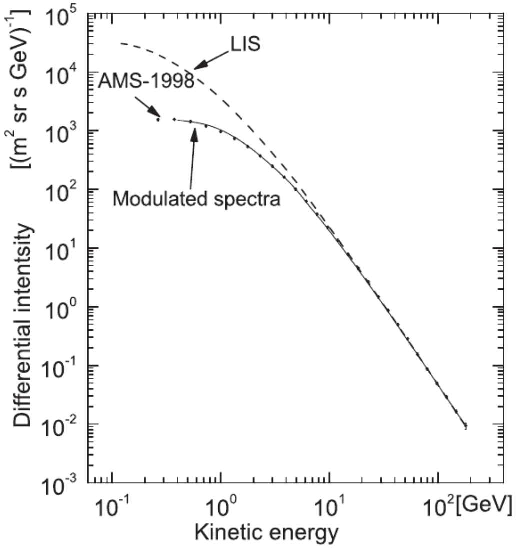

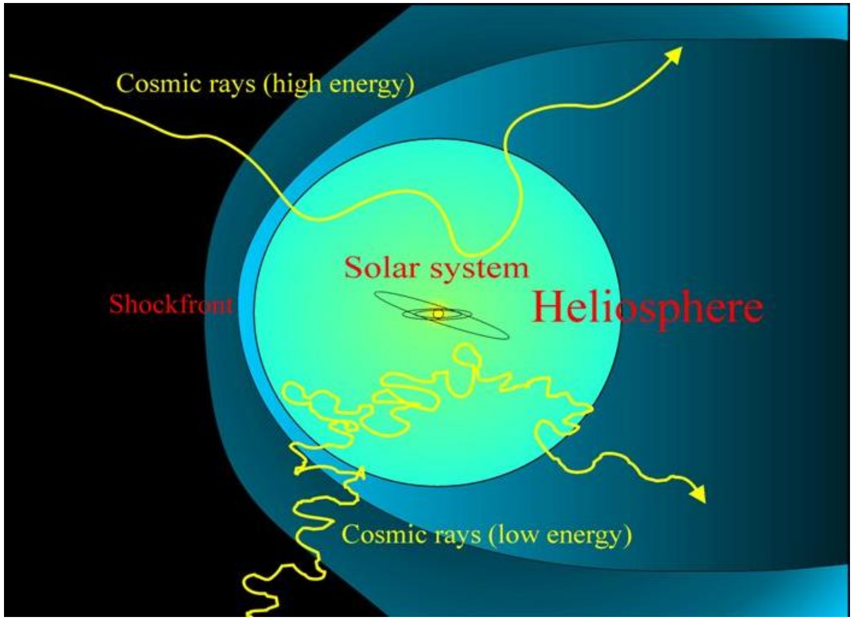

Transport through heliosphere

equation

- Propagation in the heliosphere was described by Parker (1965) equation

$$\frac{\partial f}{\partial t} = \frac{\partial}{\partial x_i}\left[\kappa_{ij}^{(S)}\frac{\partial f}{\partial x_j}\right] - \mathbf{U}\cdot\nabla f - \mathbf{V}_{\mathbf{d}}\cdot\nabla f + \frac{1}{3}\nabla\cdot\mathbf{U}\left[\frac{\partial f}{\partial \ell n p}\right] + Q$$

Diffusion
Small scale magnetic field irregoularity

Convection
Presence of the solar wind moving outward from the Sun

Drift
Large scale structure of magnetic field (e.g. gradients, curvature)

Energy change
Due to adiabatic expansion of the solar wind

Source
within helioshere

- f(r,R,t) – number of charged particles per unit volume of phase space
- Magnetic rigidity R
- **Gyroradius r_g= R/ cB**.

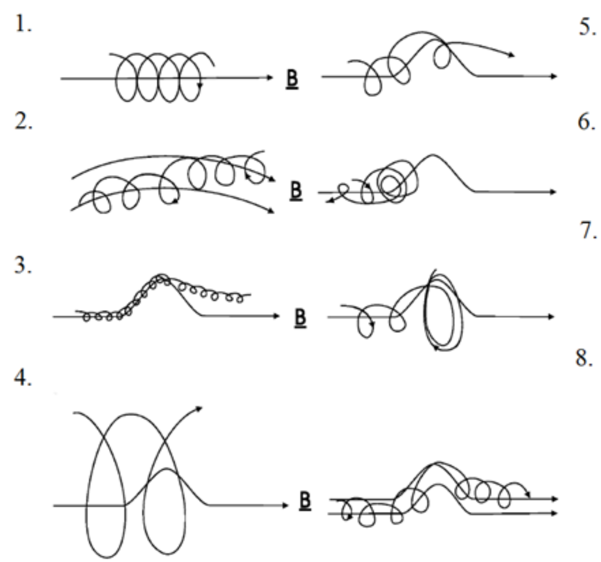

Transport through heliosphere

Equation

$$\frac{\partial f}{\partial t} + \nabla \cdot (Vf - K \cdot \nabla f) - \frac{1}{3}(\nabla \cdot V)\frac{\partial f}{\partial lnp} = q$$

- Scattering of cosmic rays by turbulence is described by the cosmic-ray diffusion tensor
- the diagonal elements describe diffusion of particles parallel $K_{\parallel}$) and perpendicul $K_{\perp}$) to the mean magnetic field,
- off-diagonal, antisymmetric terms (K_A) describe effects of gradient and curvature drift

$$\mathbf{K} = \begin{pmatrix} K_{\perp} & K_A & 0 \\ -K_A & K_{\perp} & 0 \\ 0 & 0 & K_{\parallel} \end{pmatrix}$$

Solar activity

Sporadic events

- Violent processes at the Sun produces disturbance of the heliosphere.
- This disturbance interact with geomagnetic field.
- This interaction have disruptive potential on our civilization.

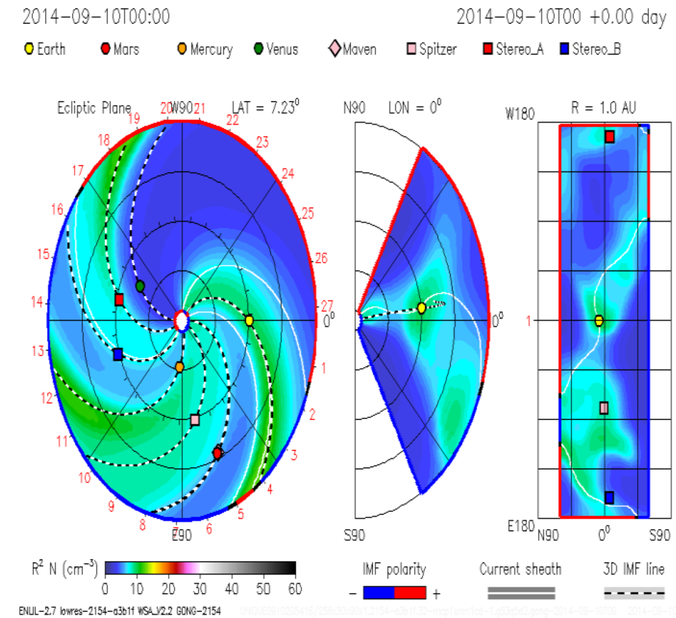

Solar activity

Type	Amplitude	origin
Periodic variations		
11-years and 22-years	Up to 30%	Solar cycles (change of sunspot number)
27-days	< 2%	due to Sun’s rotation
daily	0,5 %	flux anisotropy due to Earth’s movement through heliosphere
Sporadic variation		
GLE	Up to 300%	additional flux of charged particles from CME
Forbush decrease	~10%	decrease due to reflection of low energy CR from the shockwave in heliosphere

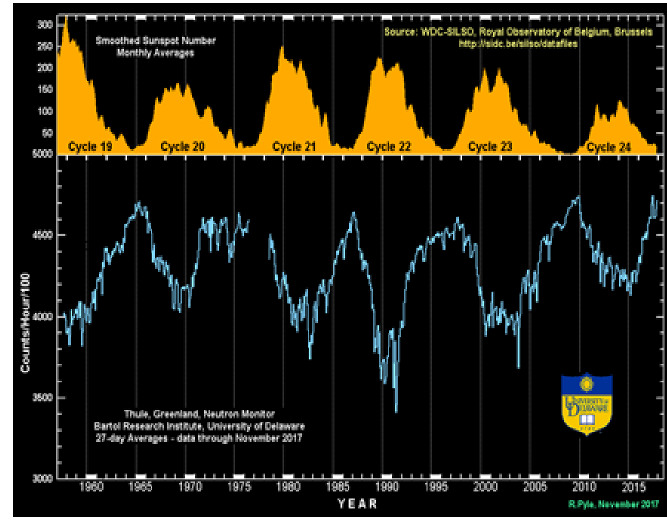

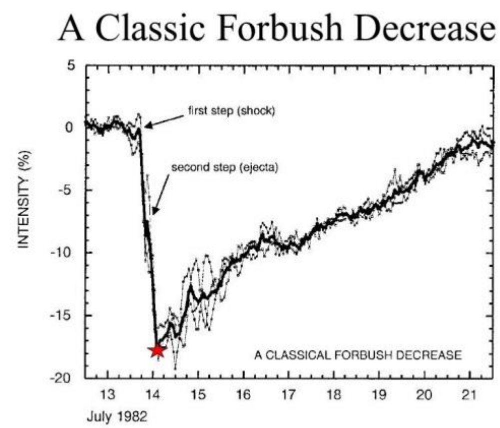

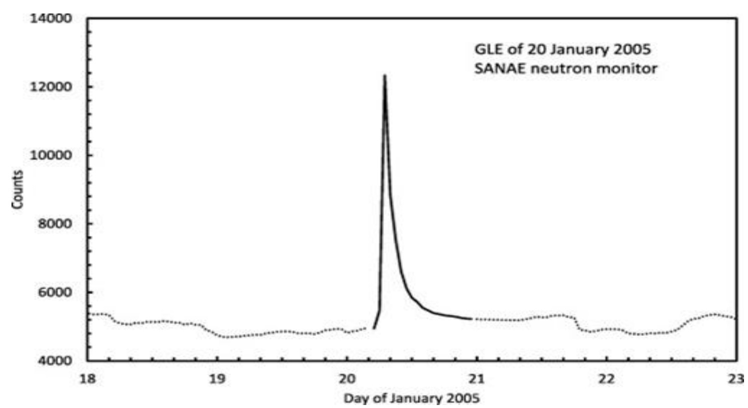

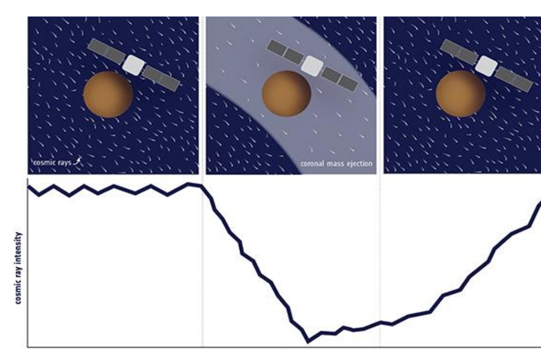

Transport through geomagnetic field

- Geomagnetic field also affect CR
- Dipole aproximation
- **R_s** (geomagnetic cutoff rigidity)
  - Smallest rigidity for charged particle to reach surface

$$R_c = \frac{M \cos^4 \lambda}{4\, r^2}$$

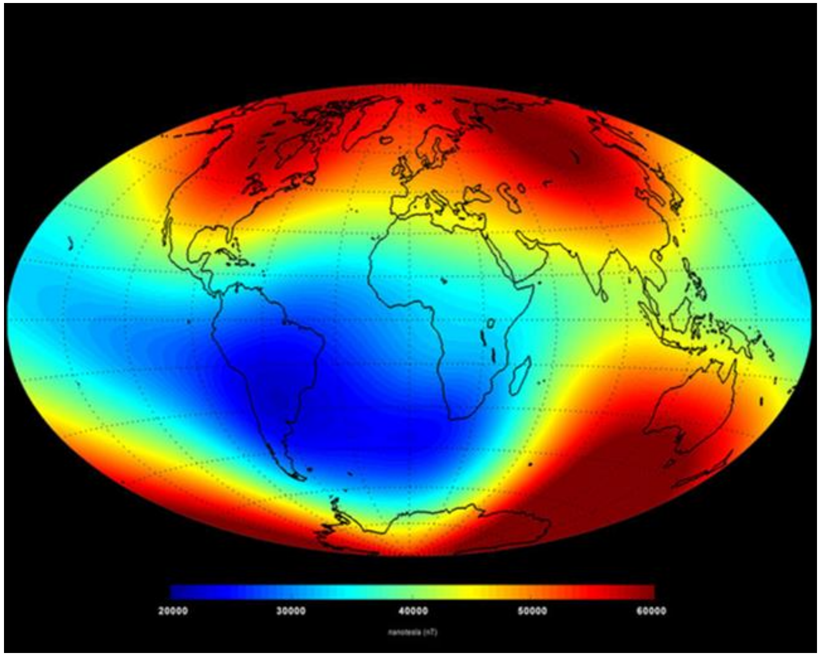

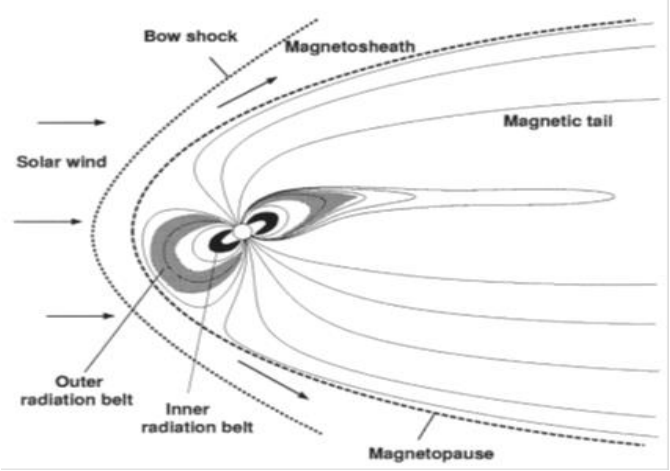

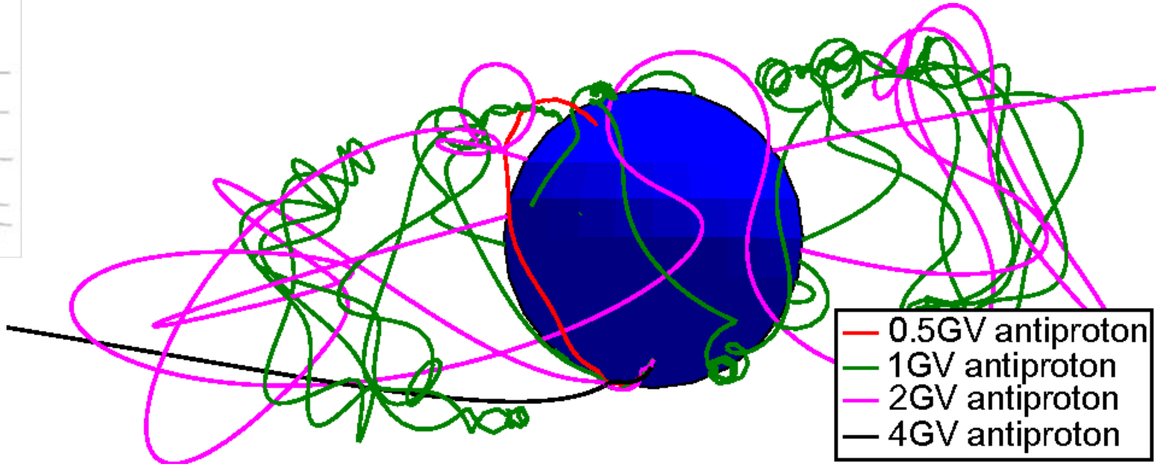

Interaction with atmosphere

Secondary CR

- Primary CR interact with nuclei from atmosphere
- ***Secondary CR shower***
  - Particles that are created from the interaction

- Electromagnetic cascade
  - $\pi^0 \rightarrow 2\gamma$
  - $\gamma^* \rightarrow e^- + e^+$ pair production
  - $e \rightarrow e + \gamma$ bremsstrahlung
- Hadronic and mesonic cascade
  - $p + p \rightarrow p + \Delta^+ \rightarrow p + n + \pi^+$
  - $\pi^+ \rightarrow \mu^+ + \nu_\mu$
  - $\pi^- \rightarrow \mu^- + \nu_\mu$
- Shower spread with every new generation of particles
- Must be corrected with atmospheric parameters in mind

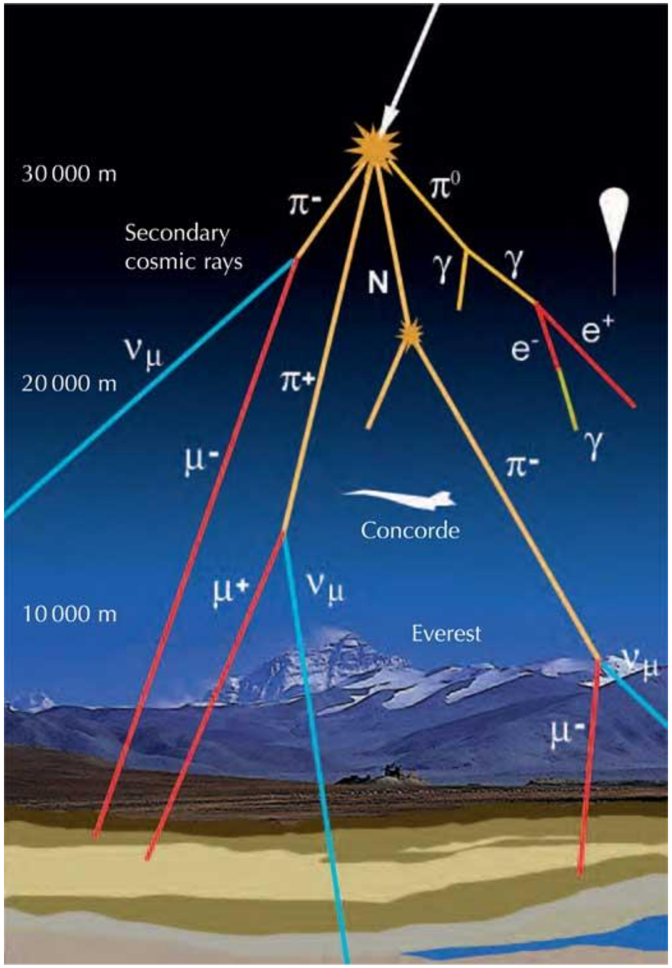

Interaction with atmosphere

Correction

- Correction on pressure
  - β barometric coefficient

$$\left(\frac{\delta I}{I}\right)_P = \beta \cdot \delta P$$

- Correction on temperature
  - Muons are more affected
  - Negative temp. effect
  - Positive temp. effect

$$\left(\frac{\delta I}{I}\right)_T = \int_0^{h_0} \alpha(h) \cdot \delta T(h) \cdot dh$$

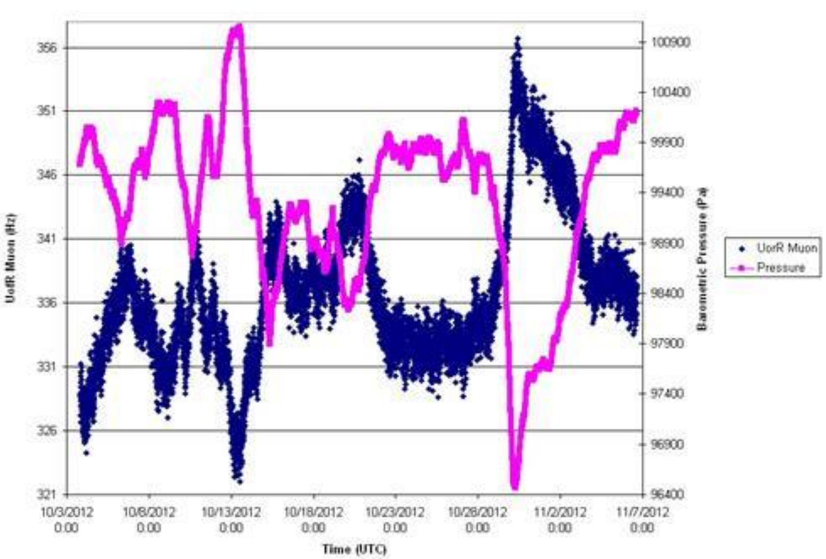

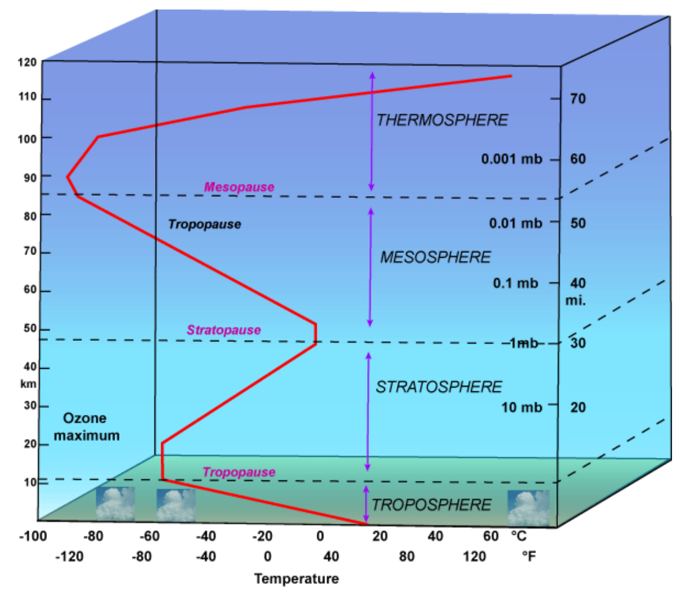

Detection of CR

Can be:

- Outside the heliosphere (Voyager)
- Above the atmosphere (various satellites)
- High in the atmosphere (high altitude balloons)
- On ground (secondary CR)
- Underground (secondary muons, neutrinos…)

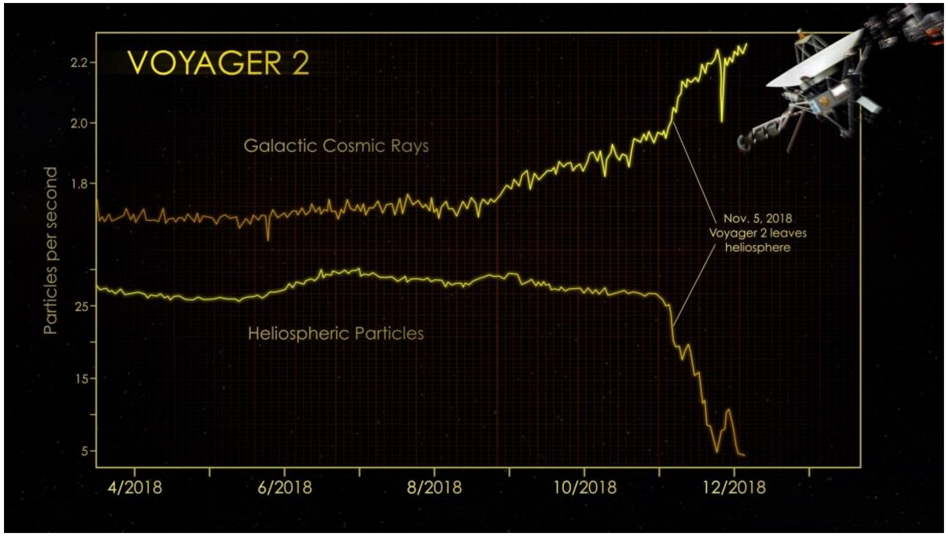

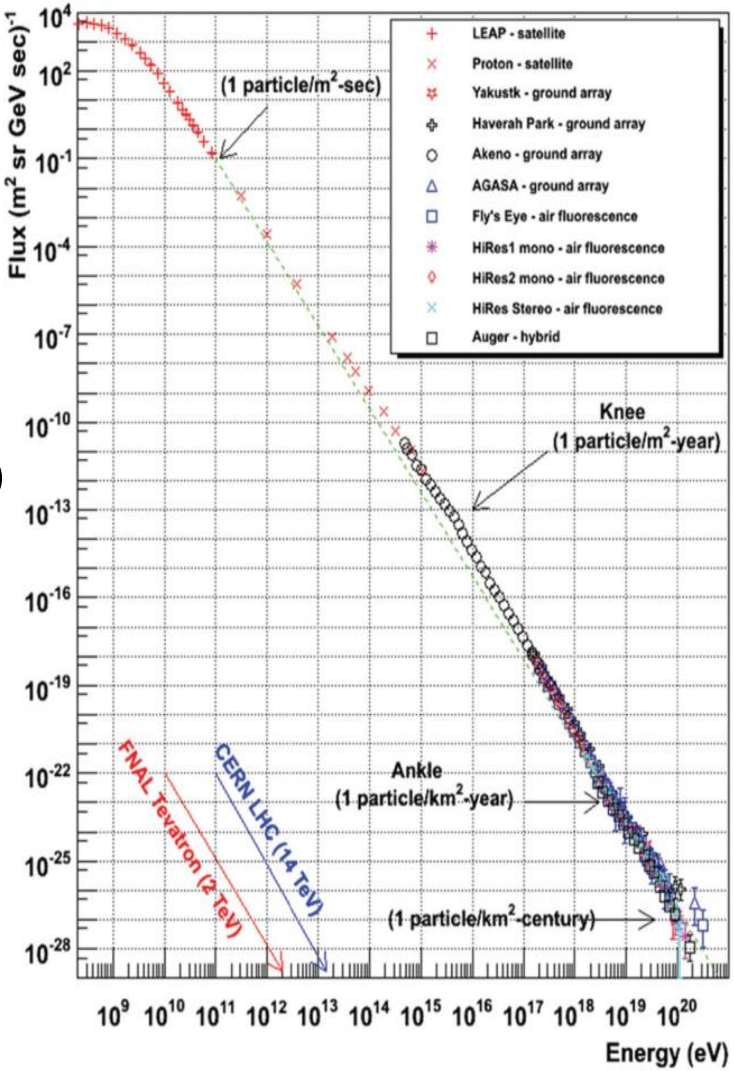

Ground systems

- Various methods are used to detect CR
- Some indirect methods includes measurement of concentration of cosmogenic radioisothopes ^{10}Be and ^{14}C in a sample
- Neutron monitors are standard detectors for ground measurements

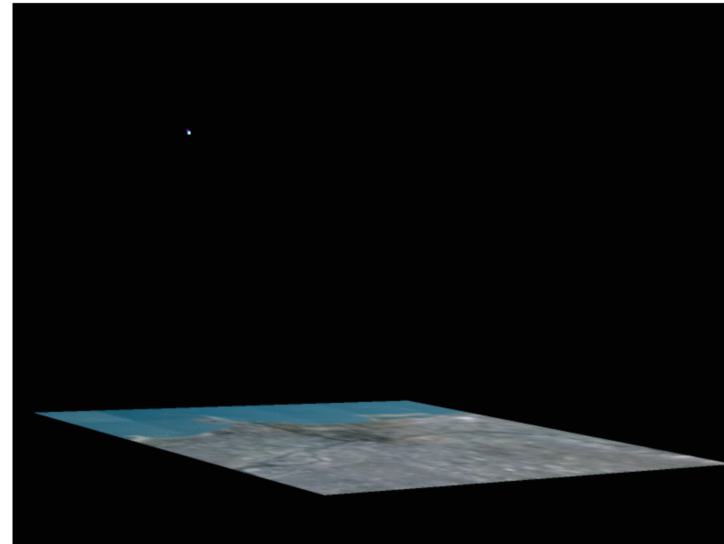

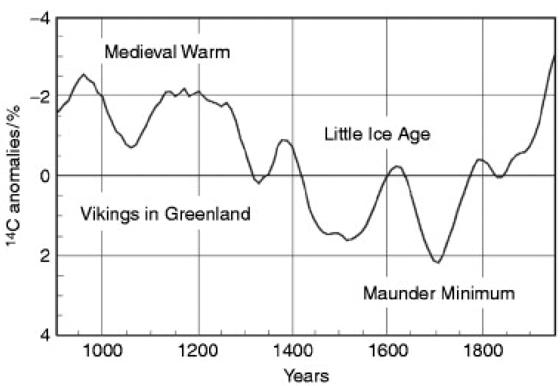

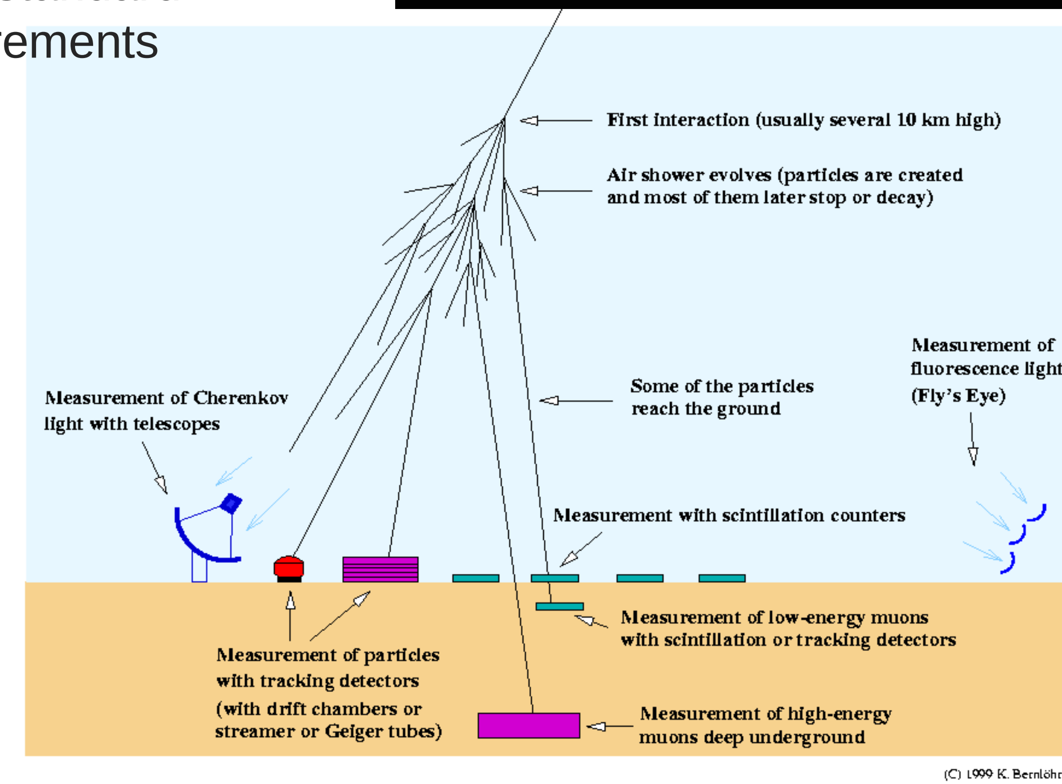

Ground systems

- Modulation effects have been studied extensively by the neutron monitors sensitive up to several tens of GeV, depending on their geomagnetic location and atmospheric depth.
- Muon detectors at ground level are sensitive to primary particles of higher energies than NMs.
- Underground muon detectors correspond to even higher energy primaries. For this reason muon observations complement NM observations in studies of long-term CR variations, CR anisotropy and gradients or rigidity spectrum of Forbush decreases

The Belgrade group

- The **Institute of Physics Belgrade** (IPB) is the reference institution for research in physics in Serbia. IPB currently employs 120 senior researchers and 80 PhD students and post-doctoral researchers.

- IPB researchers make up 1% of Serbia's research sector, producing roughly 10% of the country's scientific output.

- IPB leads Serbian participation in international projects and collaborations. The majority of the international collaborations are within the European Research Area (ERA) or with key international research centres such as CERN.
- Particle and nuclear physics research at IPB is conducted through two research groups:
  - High energy physics group – ATLAS collaboration
  - Nuclear physics group – cosmic-ray muon measurements, MICE collaboration
- IPB's Scientific computing laboratory is a part of the GRID international infrastructure.
- IPB also has a well established cooperation with JINR in Dubna.

Low-background laboratory for nuclear physics

Institute of physics, Belgrade, Serbia

- 78 m a.s.l., Geographic coordinates 44º 51’ N, 20º 23’ E
- Minimal vertical rigidity 5.3 GV.
- Consist of two parts:
  - Ground level (GLL)
  - Underground (UL) level, dug in 12m of loess .
- Scientific research activities in the LBLNP are in the fields of nuclear and high energy physics. They are related in particular to cosmic-ray physics, nuclear spectroscopy, radon and environmental radiation measurements

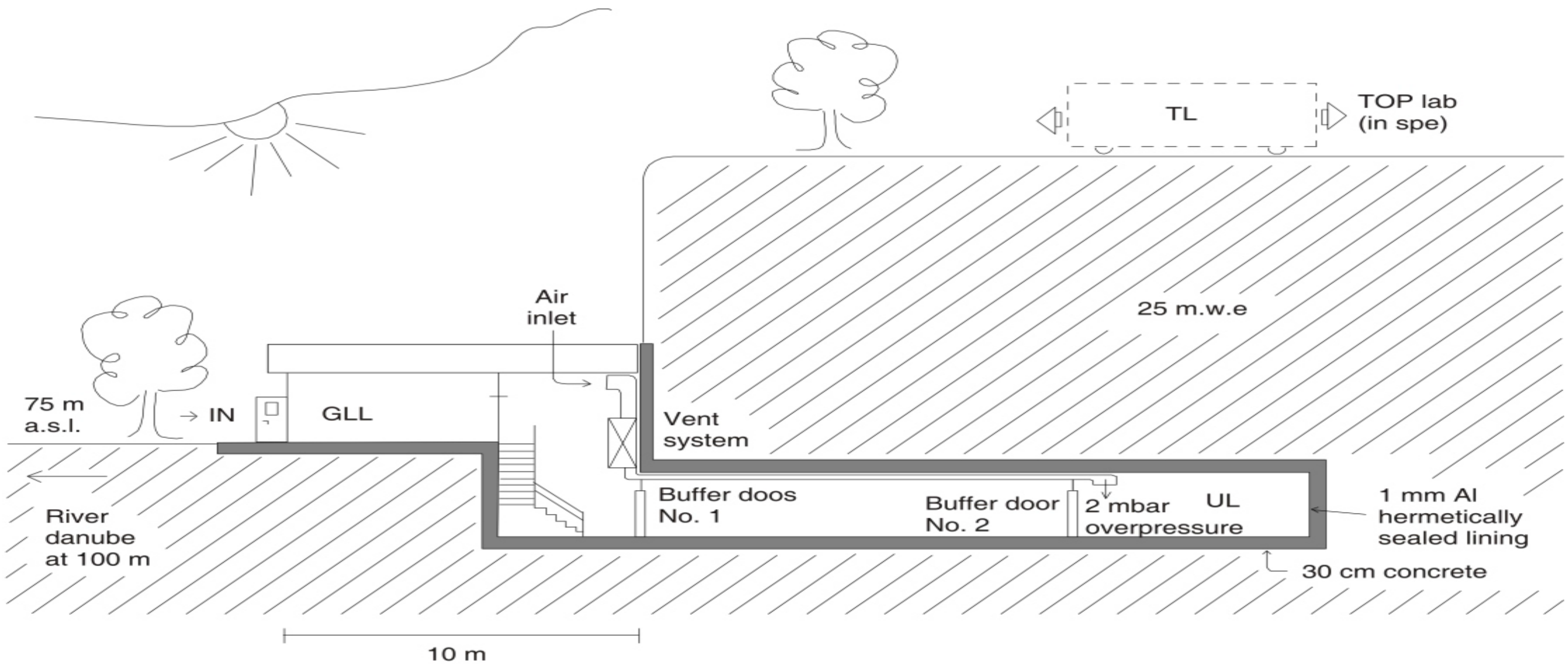

Low-background laboratory for nuclear physics

Past activities

- For the last 25 years we participated in the realization of LOREX (lorandite experiment), the only geochemical experiment to determine the average solar neutrino flux over the last 5 million years, via the neutrino capture by Thallium-205.
- Studying rare nuclear and particle processes
- Comprehensive studies of all components of background in high sensitivity experiments
- Cosmic ray muon induced signatures in low-energy detectors
- Continuous monitoring of cosmic ray muon intensity (from 2002)
- Radon and enviromental radiation studies
- Neutron induced nuclear reaction
- Backgroundless search for element Z-113 (eka-thallium) in nature: (conc<e-11g/g at 90%CL)
- Plasma focus-fusion machine
- etc...

$$^{205}\mathrm{Tl} + \nu_e \longrightarrow {}^{205}\mathrm{Pb} + e^-$$

European Indoor Radon Map, March 2017

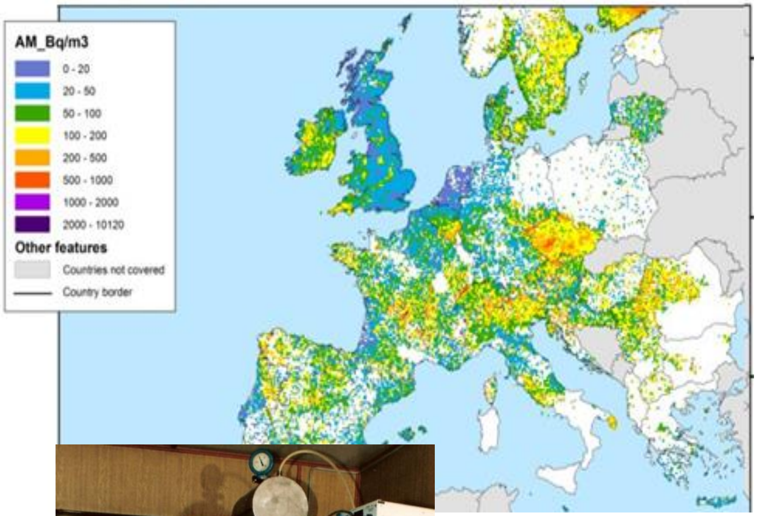

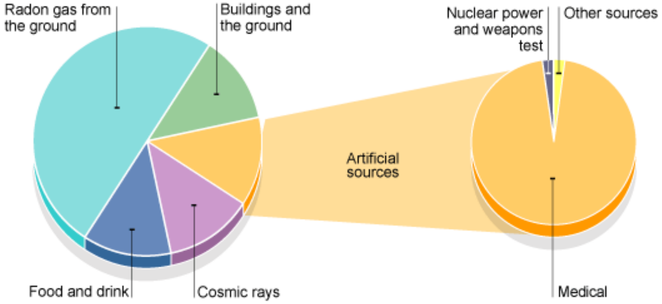

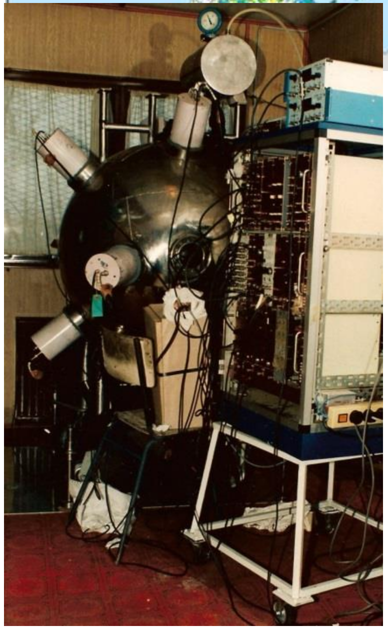

Low-background laboratory for nuclear physics

Recent collaborations

- MICE experiment. EU, EUCARD2 (2014-2017).
- Bilateral project with Belorussia
- IAEA RER9136: Reducing Public Exposure to Radon by Supporting the Implementation and Further Development of National Strategies
- Belgium. CHANDA (solving CHAllenges in Nuclear Data) project. FP7-EURATOM-FISSION program.
- EUFRAT (European Facilities for Nuclear Reaction and Decay Data Measurements) program. JRC-European Commission:
  1. Prompt-fission gamma ray characteristics from the reactions 235U(n,f) in the resolved neutron-resonance region
  2. Set up and commissioning of a CeBr3 array as part of the GLADIS hybrid gamma-ray spectrometer.

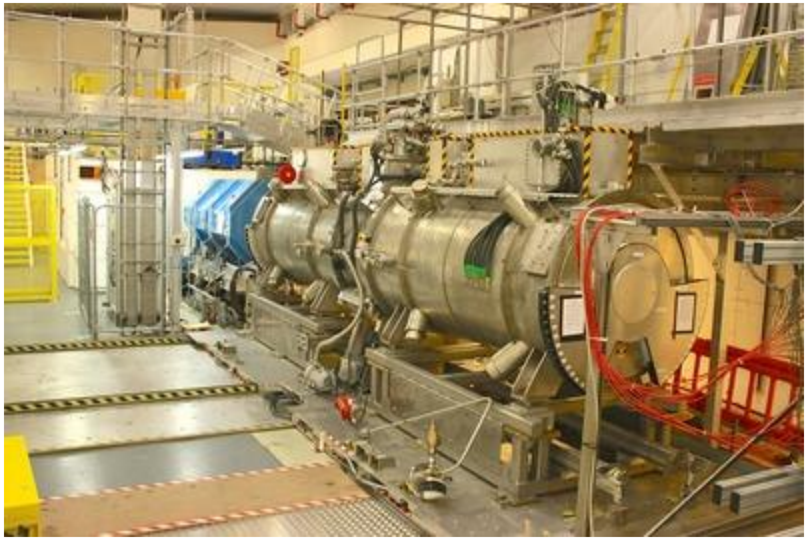

Low-background laboratory for nuclear physics

Experience in high energy physics

- CMS experiment at CERN, 2003-2010
- NA61/SHINE experiment at CERN, 2011-2015
- MICE experiment at RAL, since 2015
  - software development, MC simulations (Geant4)
  - data processing and calibration, data transfers in grid environment
  - analyses (also utilizing the artificial neural network approach or multivariate analysis)
  - operations: NA61 ToF detectors M&O, CMS Ecal Safety System M&O

Low-background laboratory for nuclear physics

Cosmic rays physics

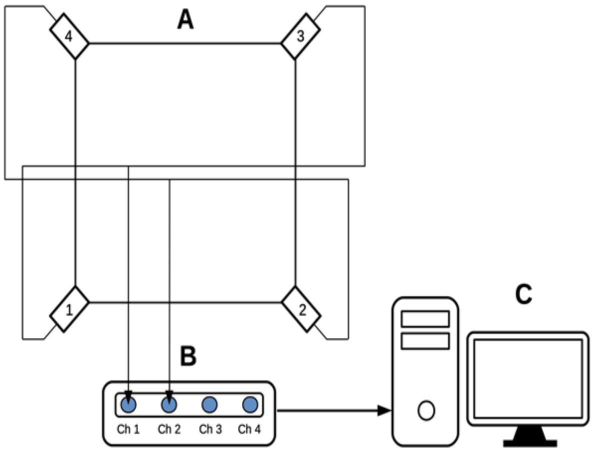

- The experimental setup consists of two identical sets of detectors and read out electronics, one situated in the GLL and the other in the UL. Each setup utilizes a plastic scintillation detector with dimensions 100cm × 100cm × 5cm equipped with 4 PMTs optically attached to beveled corners of a detector.
- Preamplifier output of two diagonally opposing PMTs are summed and fed to a digitizer input (CAEN FADC, type N1728B). FADC operates at 100MHz frequency with 14 bit resolution.
- They are capable of operating in the list mode, when every analyzed event is fully recorded by the time of its occurrence and its amplitude. This enables correlation of the events, both prompt and arbitrarily delayed, at all four inputs with the time resolution of 10 ns. Single and coincident data can be organized into time series within any integrationn period from 10 ns up. The two N1728B units are synchronized, enabling coincidence/correlation of the events recorded in both of them. The flexible soft ware encompassing all above said off-line analyses is user-friendly and entirely homemade.

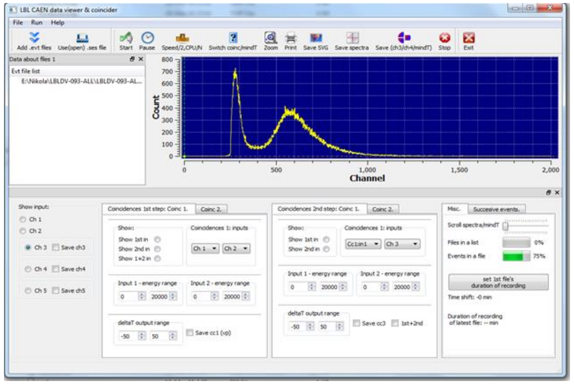

Low-background laboratory for nuclear physics

Cosmic rays physics

- The events generating enough scintillation light to produce simultaneous signals in both inputs, exceeding the given threshold, are identified as muon events.
- To account for the contribution from other particles to the experimental spectrum, not all the events in the spectrum are counted when muon time series are constructed.
- Muon events are defined by setting the threshold corresponding to muon fraction of recorded spectrum. Threshold is set in terms of "constant fraction" of the spectrum maximum, which also reduces count rate fluctuations due to inevitable shifts of the spectrum during long-term measurements.

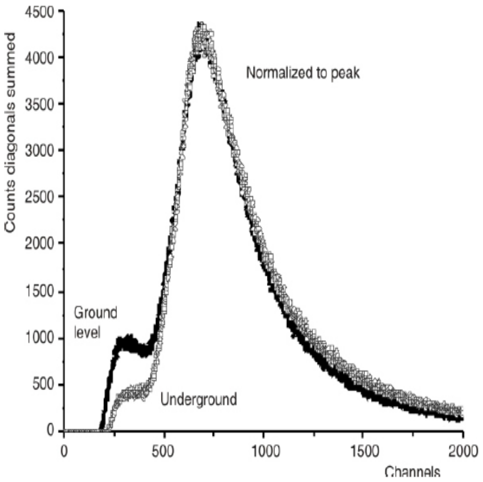

Figure 9. The sum spectra of two diagonals of the large plastic detectors in the UL and GLL. For comparison, the spectra are normalized for the peaks to coincide. Channel 650 now corresponds to the muon energy loss of 10 MeV. The integral of this peaked distribution is taken as the first approximation to the CR muon count by the large detectors

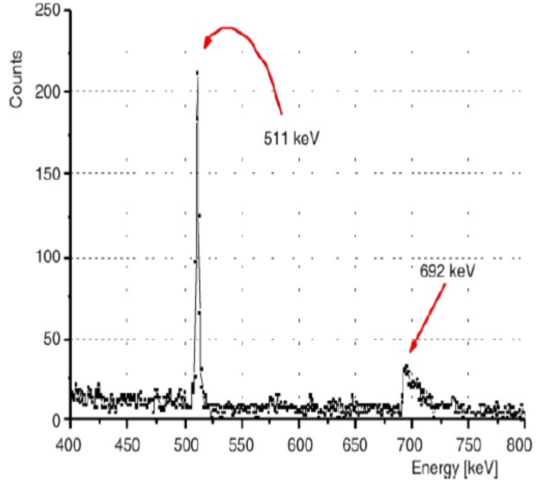

Figure 11. The portion of the background of the HPGe spectrum coincident with the large plastic detector with delays in the range of 1 to 5 μs, after 187 days of measurement time. It shows the annihilation line which is due to the decays of positive muons stopped in the lead castle, and the triangular structure at 692 keV, which is due to inelastic scattering of fast neutrons on 72-Ge, the neutrons originating mostly from direct fast muon interactions with nuclei and certainly less from captures of stopped negative muons. The threshold in this spectrum is sufficiently high to leave this last structure unscathed

Low-background laboratory for nuclear physics

Simulation packages

- For the simulation of cosmic radiation the CORSIKA software package developed for the experiment KASCADE was used.
- Geant4 software package has been developed for particle physics and simulates the interaction of particles with matter.It is a very good tool to simulate the response of detectors used in the experiment.
- Cosmic rays can be simulated from primary cosmic radiation that is entering in the atmosphere and follow the creation of the cascade through the atmosphere, and finally detects using plastic scintillators at the Earth's surface or in the underground laboratory.

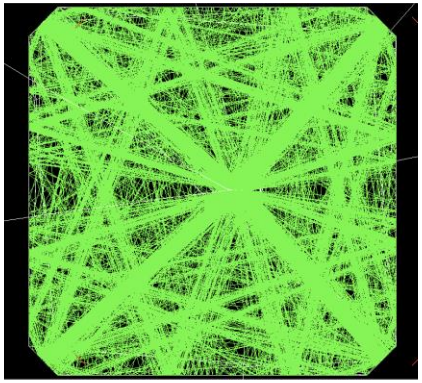

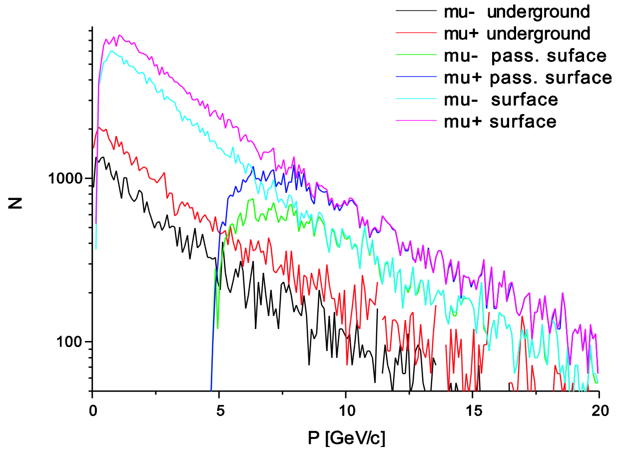

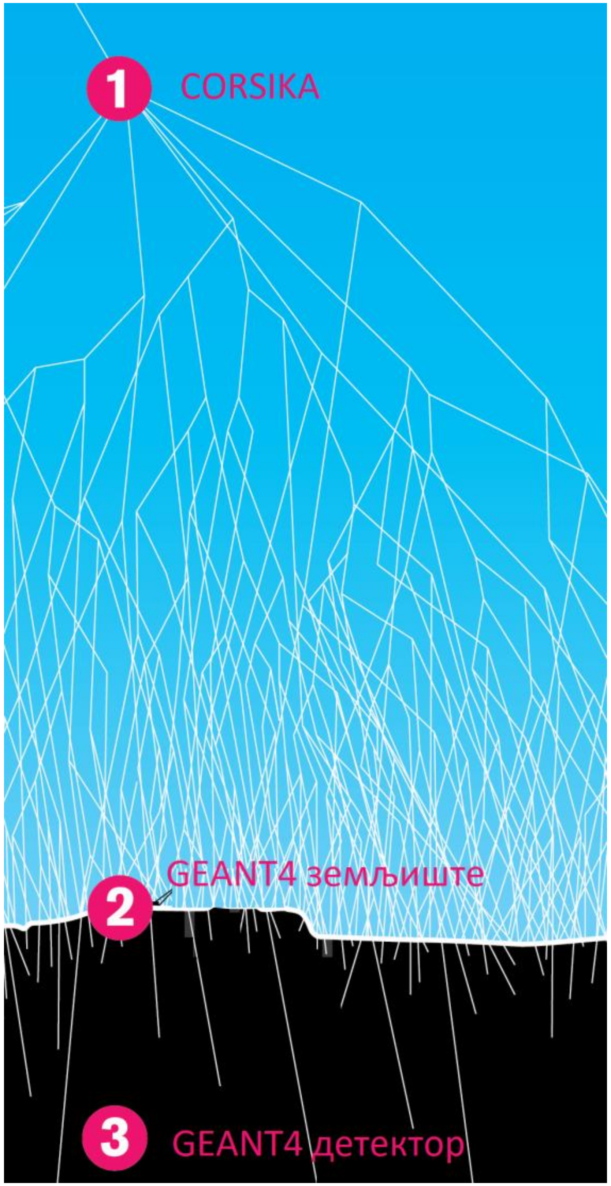

Low-background laboratory for nuclear physics

Simulation packages

- Response of the detectors are calculated from simulation
- Range of energy for the primary CR found

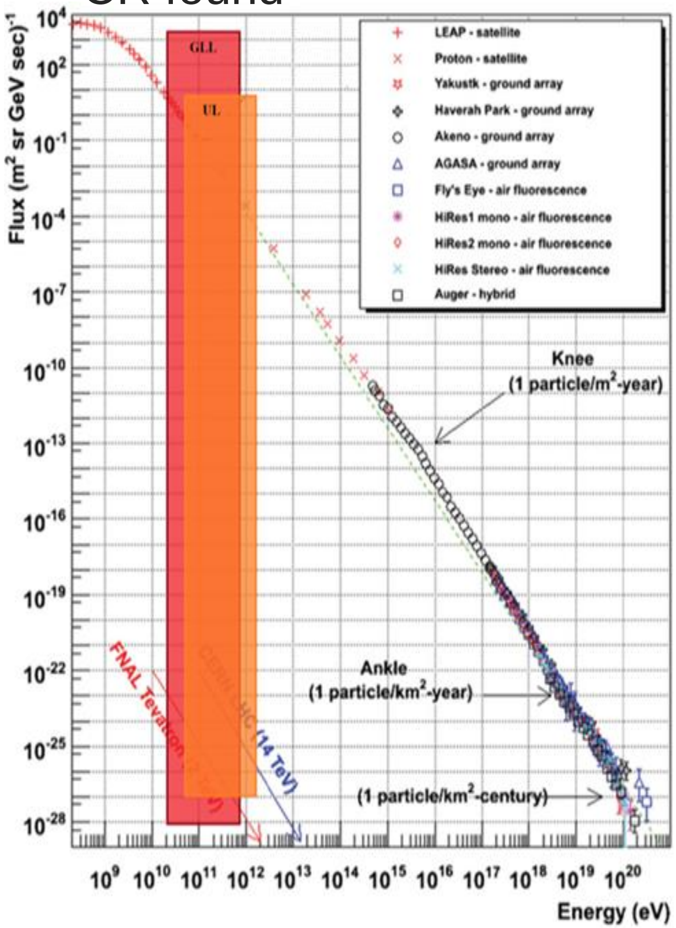

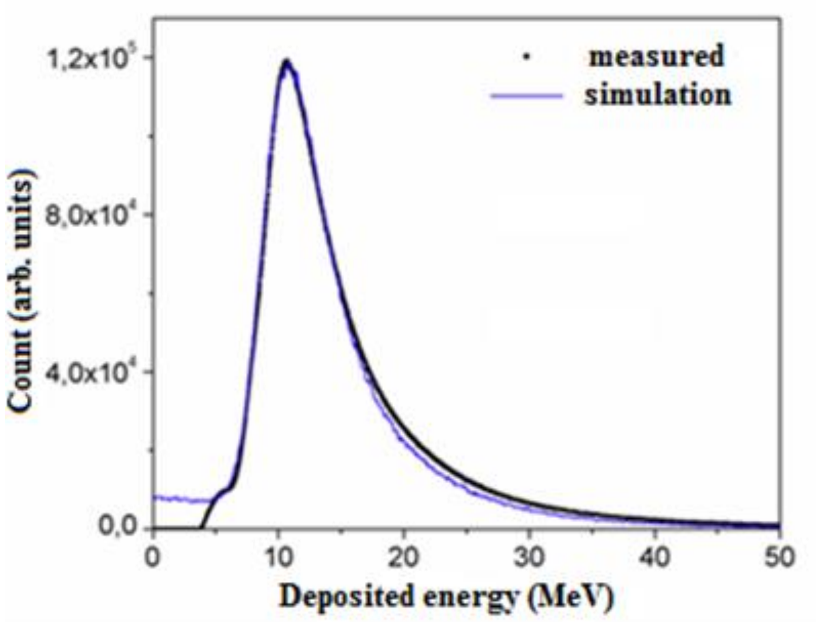

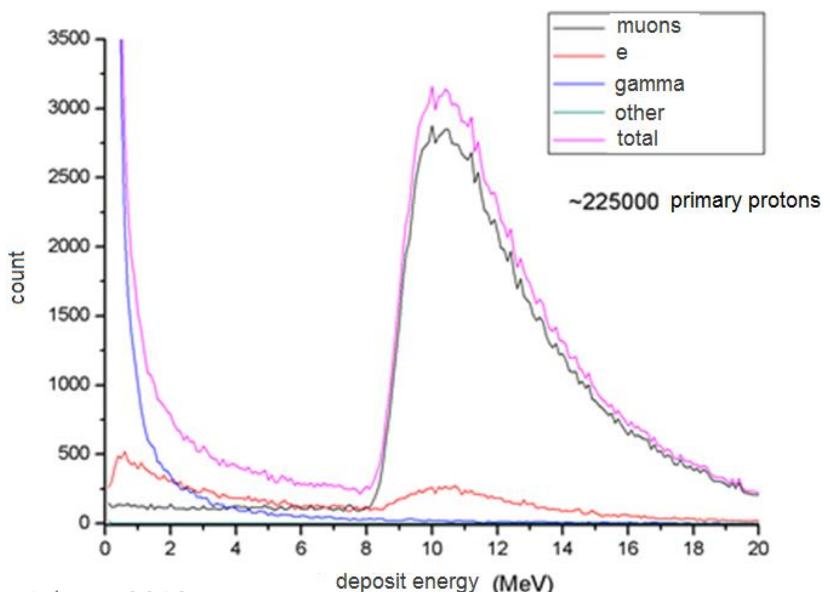

Low-background laboratory for nuclear physics

"Asymut" set-up

- **Asymmetric muon telescope** separates muons with respect to zenith angle. Asymmetric muon telescope is an inexpensive detector, constructed from the components already available in the laboratory.
- It consists of two plastic scintillators of unequal dimensions. Detectors are separated by 78 cm, to have roughly the same count rate in the **coincident** and **anticoincident** mode. Lower detector in single mode operates in the same manner as the one in the GLL, with wide angular acceptance. The coincident mode constitute the events registered in both upper and lower detector, while the anticoincident mode is made from the muons passing through the upper but not the lower detector and therefore favors inclined muon paths.

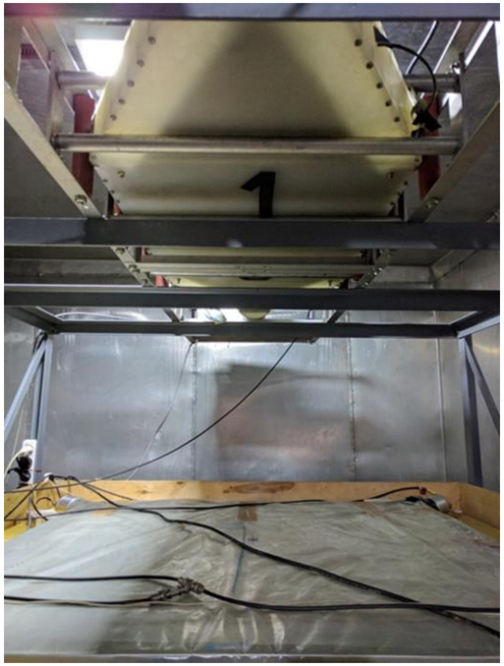

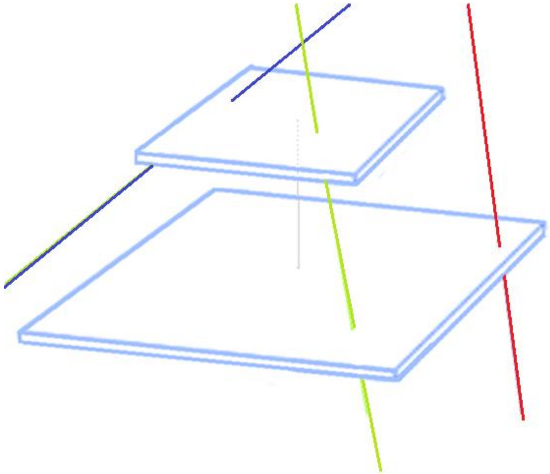

Low-background laboratory for nuclear physics

"Asymut" set-up

- Different angular distribution means different path length of muons registered in three modes of ASYMUT and also **different energy distribution** of parental primary particles
- Other experimental arrangement is also discussed –Planar configuration

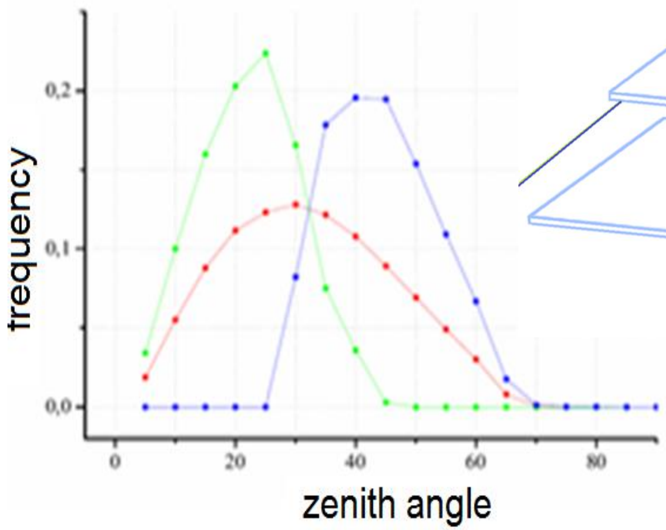

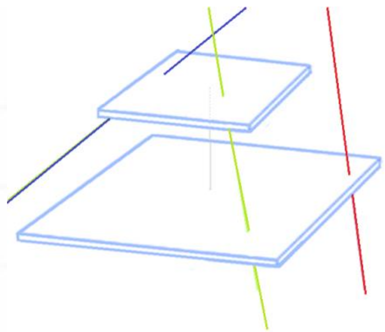

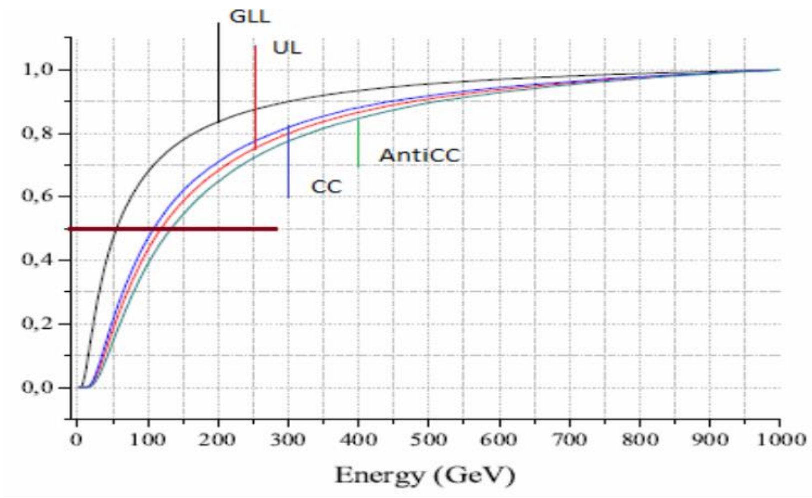

Cumulative response function to galactic cosmic rays of different muon detectors in the lab. 0.5 level corresponds to median energy.

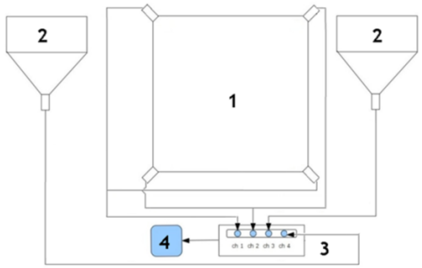

Detectors	$E_{0.05}$ (GeV)	E_{median} (GeV)	$E_{0.95}$ (GeV)
CC	27	121	1585
ANTI	35	157	2031
UL	31	137	1811

Solar activity

Ground measurements

- Comparison with nearby NM
  - The amplitude of a Forbush decrease is one of its main characteristics.

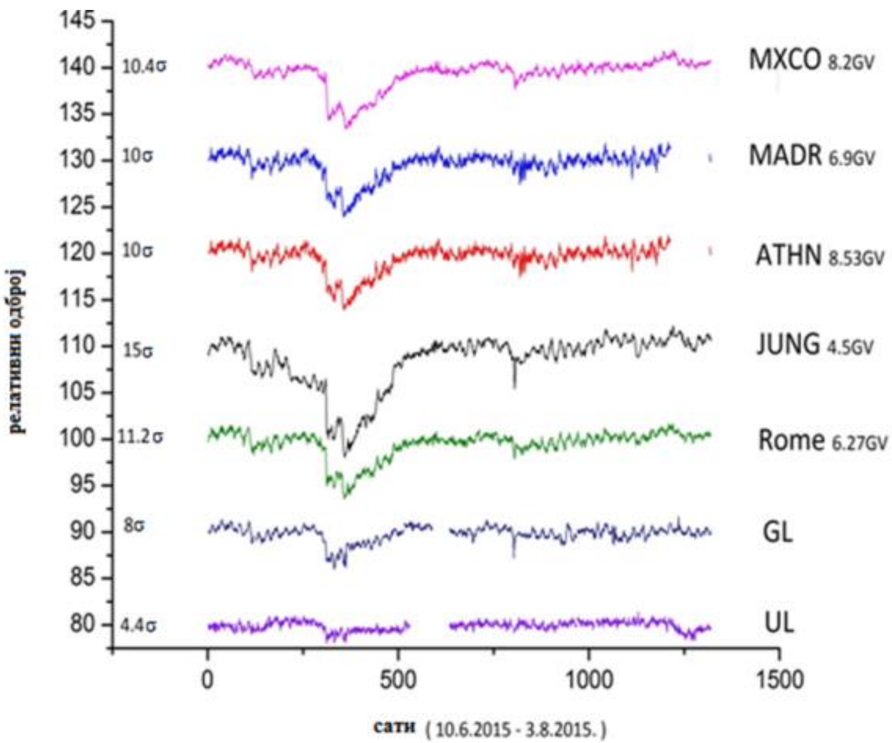

- Dependence of FD amplitude on median rigidity (or energy) is expected to follow the power law:

$$\frac{\Delta N}{N} \sim R_m^{-\gamma}$$

- γ should be ~(0,4-1,3)

Solar activity

Ground measurements

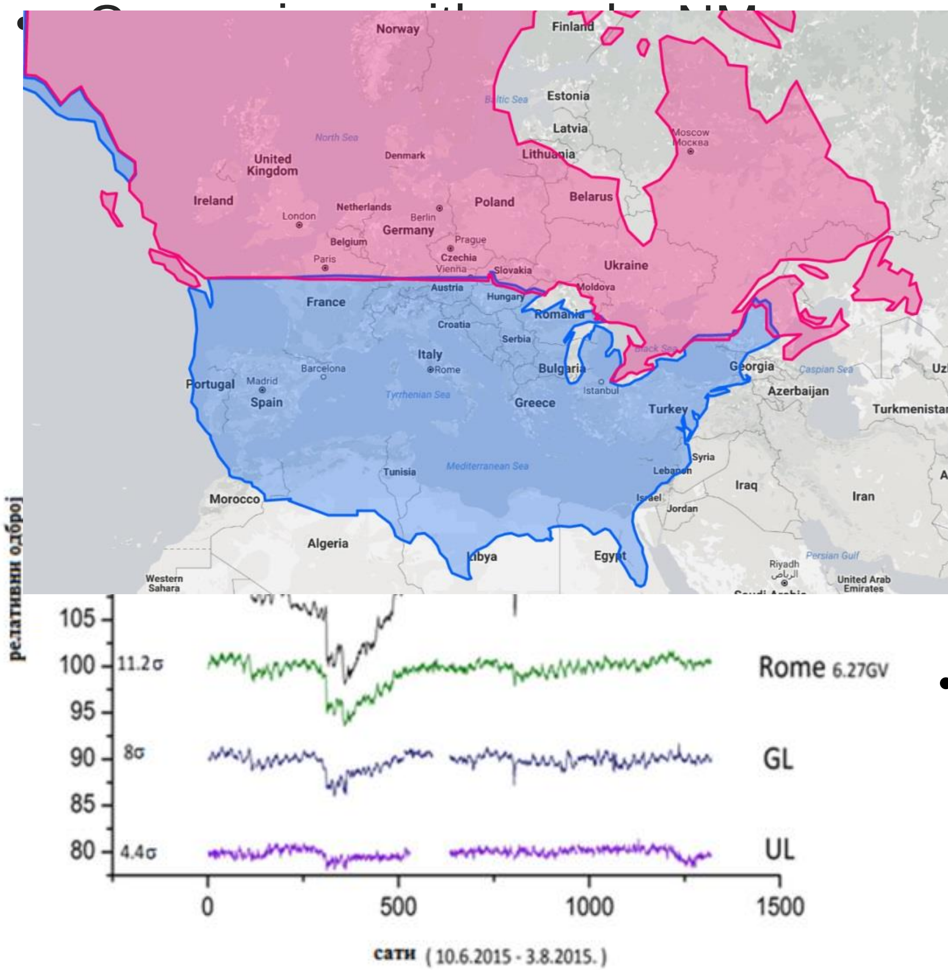

- Dependence of FD amplitude on median rigidity (or energy) is expected to follow the power law:

$$\frac{\Delta N}{N} \sim R_m^{-\gamma}$$

- γ should be ~(0,4-1,3)

Solar activity

ground measurements Forbush decrease

- As the solar activity was approaching its maximum during solar cycle 24, an X-ray flare (X5.4 class) occurred in NOAA AR 11429 at 00:02 UT on 2012 March 7 (flare onset time), associated with an intense halo CME with a peak speed of about 2684 km s−1, and followed by a smaller flare (X1.3 class) about 1.5 hr later. After that, a series of M-class flares and large CMEs occurred within the same region.
- Strong FD detected after this aperiodical solar event.

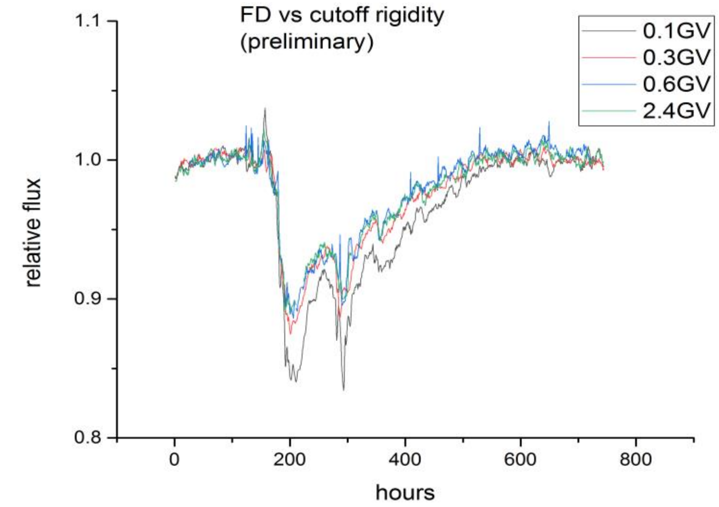

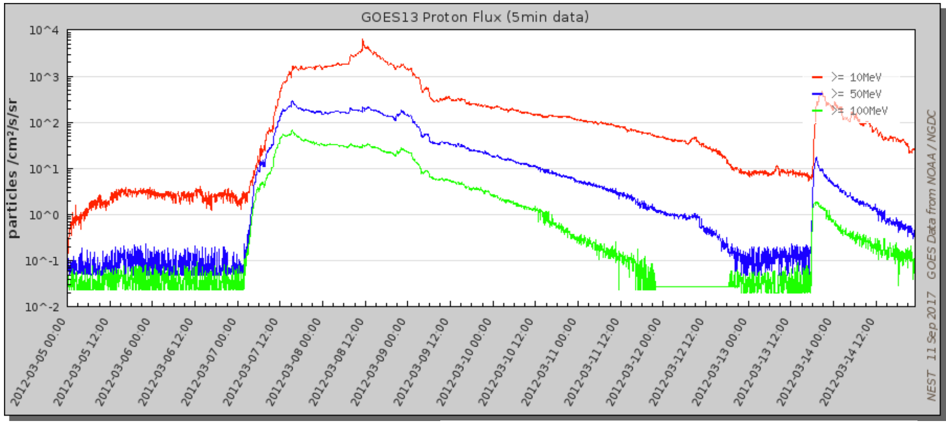

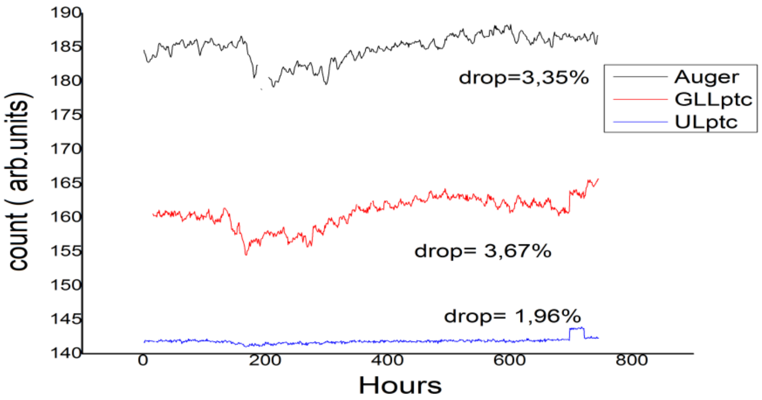

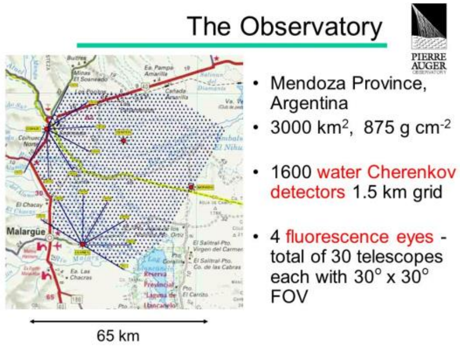

Solar activity

ground measurements Forbush decrease

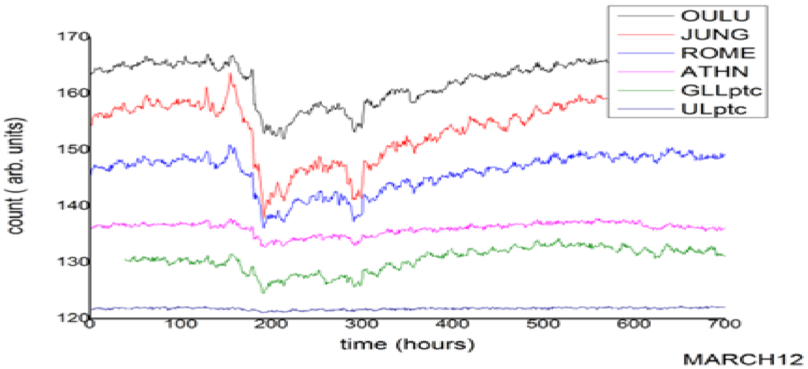

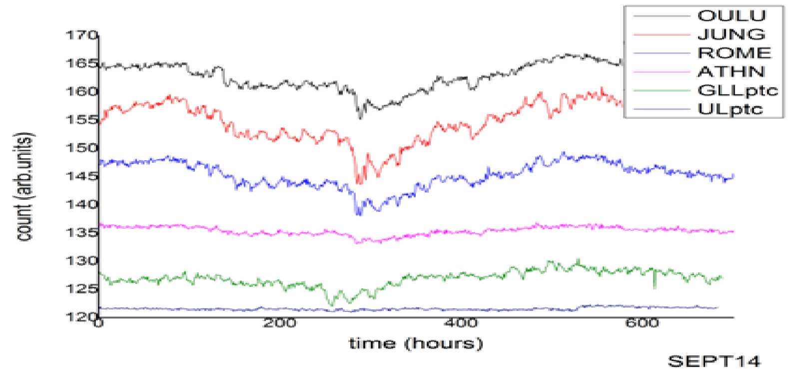

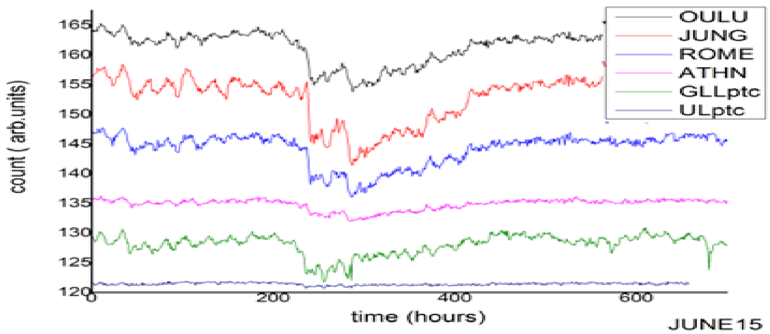

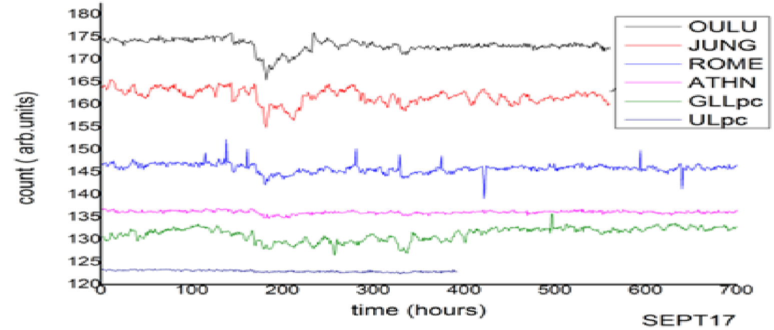

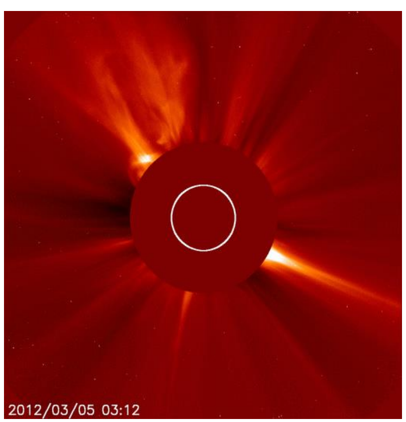

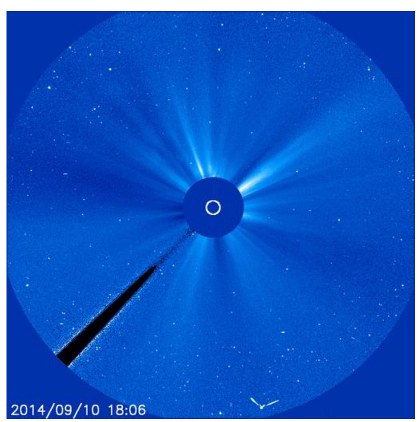

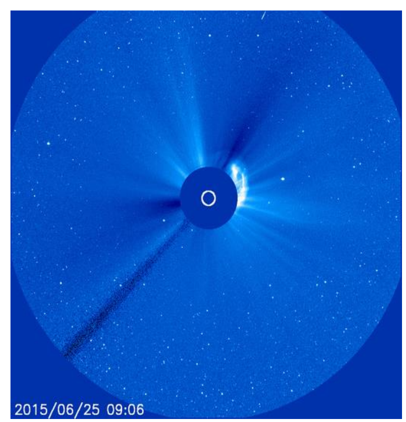

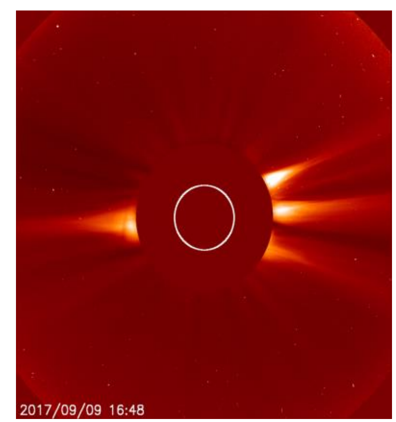

Solar activity

ground measurements Forbush decrease

- Found dependence of FD amplitude on median rigidity o illustrates applicability of our setup for studies of consequences of CR solar modulation process in the energy region exceeding sensitivity of neutron monitors.

- Amplitude of Forbush decrease is inverse proportional to component of the diffusion tensor parallel to magnetic field which depends on CR rigidity

- Higher power indices can be due to more complex variation of GCR. This more complex variation is a result of series of CMEs during this event that leads to large compound ICME structure with multiple shocks and transient flow

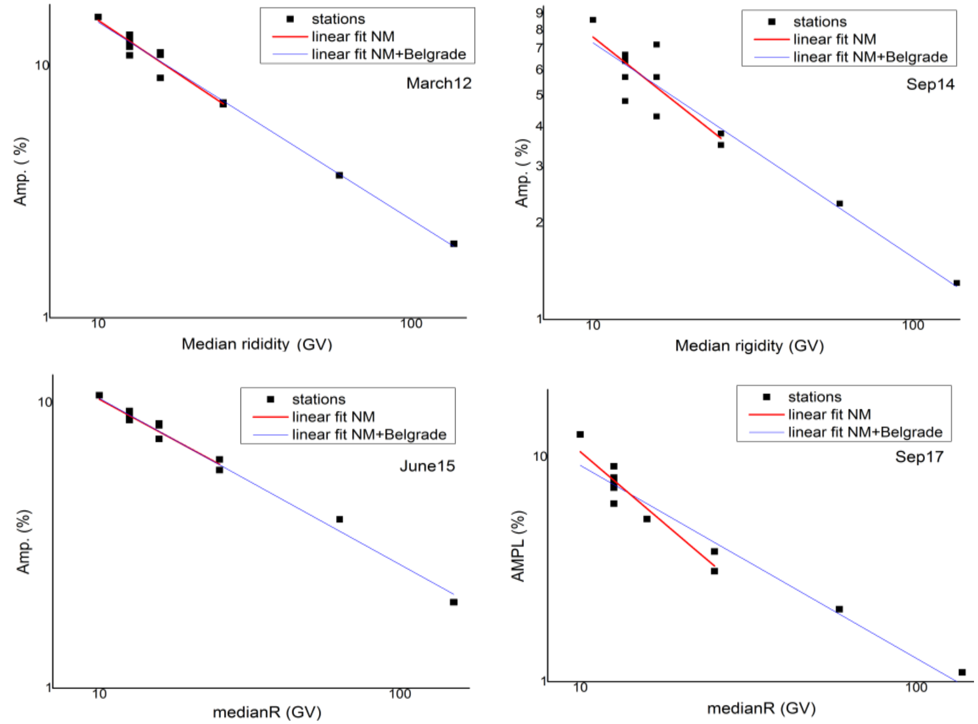

γ	NM	NM+Belgrade
March 2012.	0,82±0,08	0,78±0,03
Sept. 2014.	0,79±0,16	0,67±0,06
June 2015.	0,57±0,05	0,58±0,02
Sept. 2017.	1,27±0,16	0,86±0,07

Comparison with satellite data

- **STEREO (Solar Terrestrial Relations Observatory)**
  - Two nearly identical spacecraft were launched in 2006 into orbits around the Sun
  - Communication with STEREO B stopped 2014.

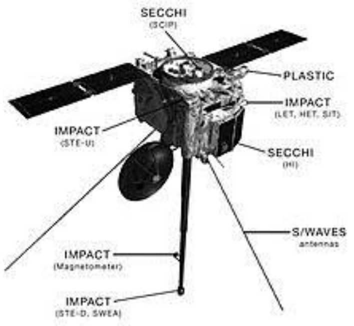

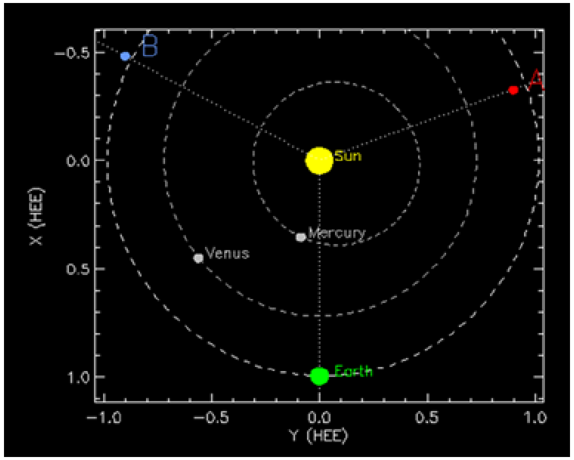

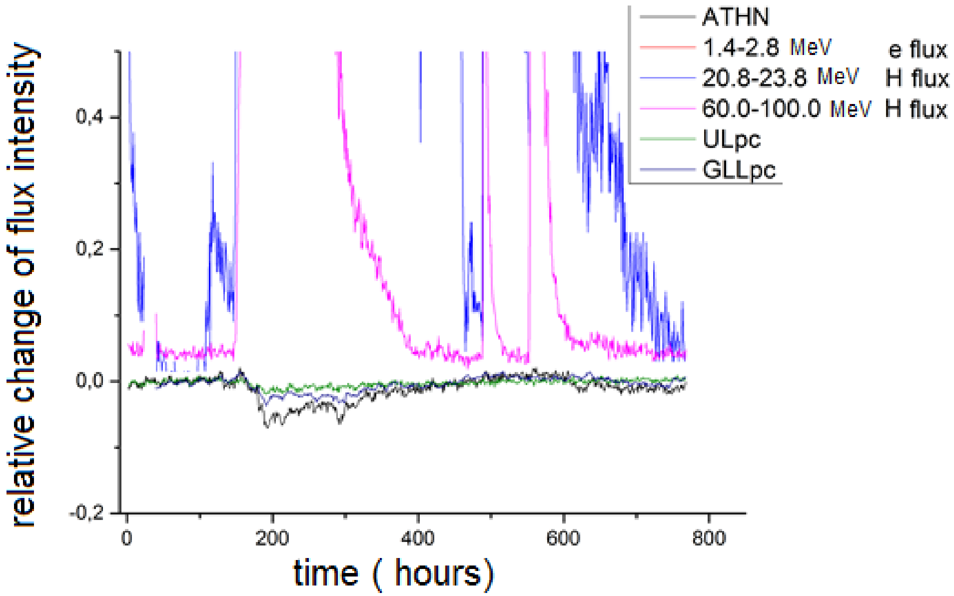

FD March 2012

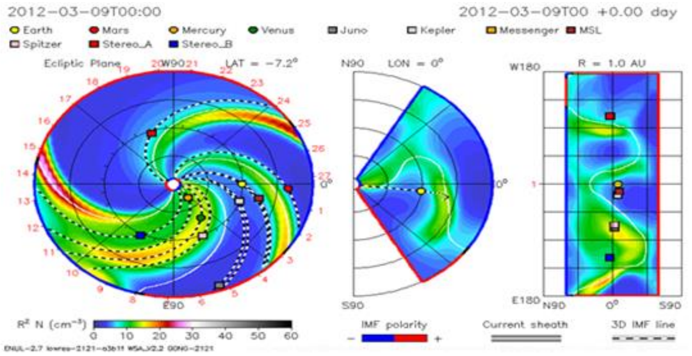

Comparison of ground and satellite data

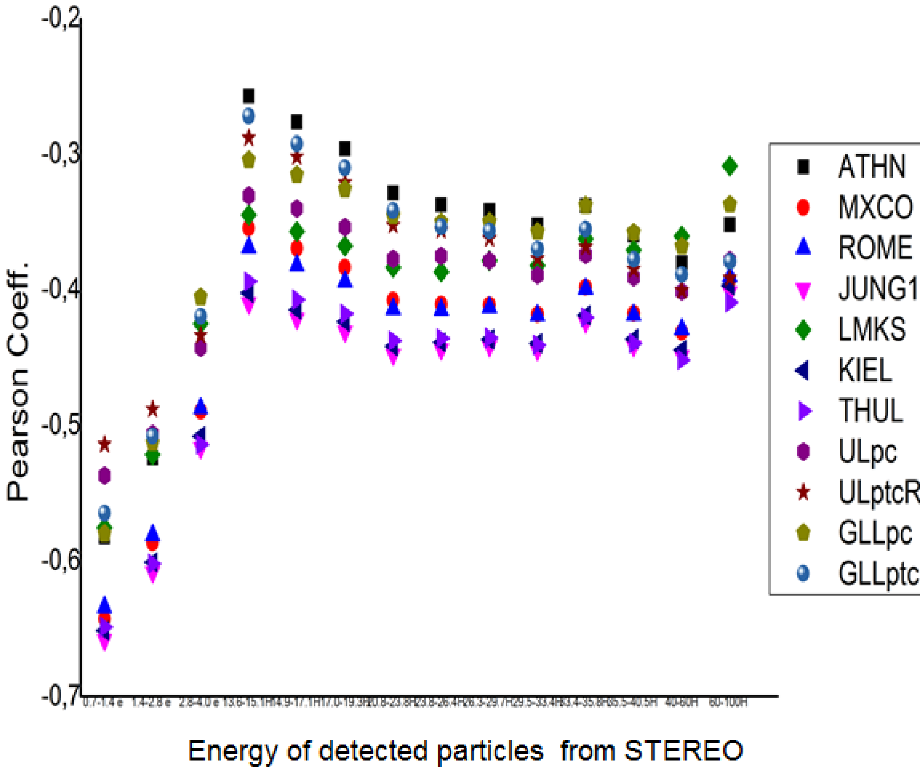

$$r = r_{xy} = \frac{\sum_{i=1}^{n}(x_i - \bar{x})(y_i - \bar{y})}{\sqrt{\sum_{i=1}^{n}(x_i - \bar{x})^2}\sqrt{\sum_{i=1}^{n}(y_i - \bar{y})^2}}$$

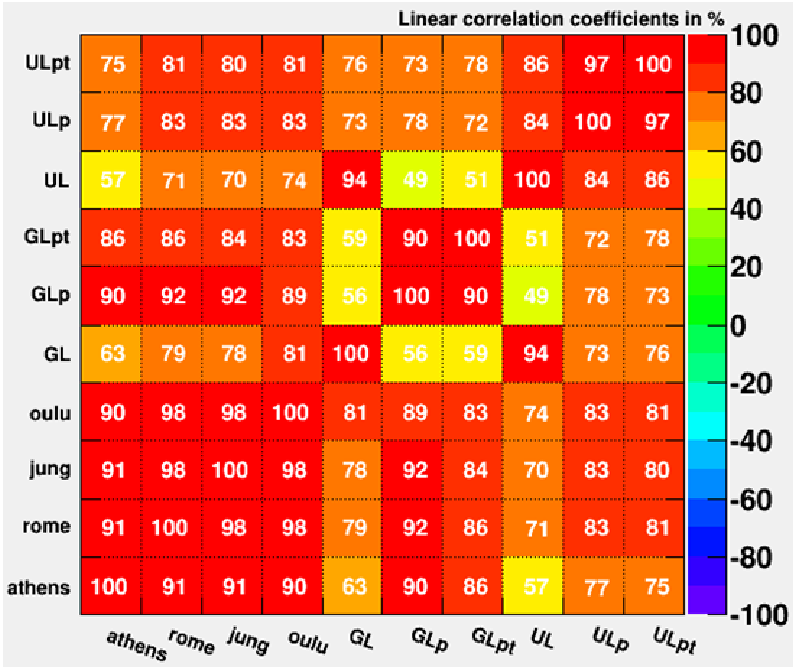

Correlation matrix of linear correlation coefficient (in %) for Belgrade cosmic ray station with its temperature and pressure corrected underground and ground level detectors (UL_tpc, GL_tpc), only pressure corrected (UL_pc, GLL_pc),raw data (UL_raw, GLL_raw) and Rome, Oulu, Jungfraujoch (JUNG) and Athens NMs for March 2012.

Muons and temperature of the atmosphere

- Common empirical models use temperature of the muon creation level in the atmosphere **for temperature corrections** but muons are created throughout the atmosphere
- Our empirical model is based on using temperature on several levels in the atmosphere.
- Use Principal component analysis to untangle these correlated parameters by switching to new set of (orthogonal) linearly independent parameters created from linear combination of original parameters.

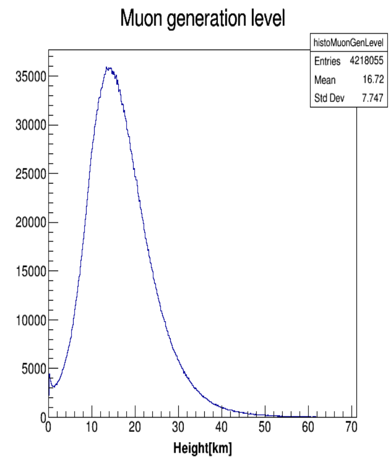

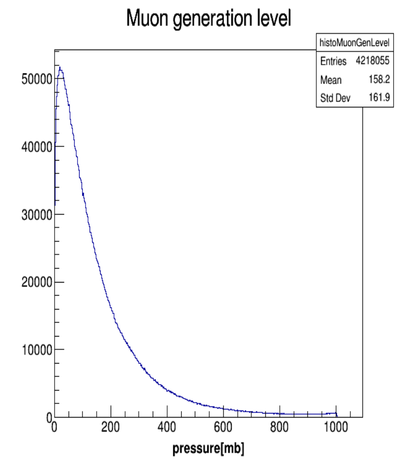

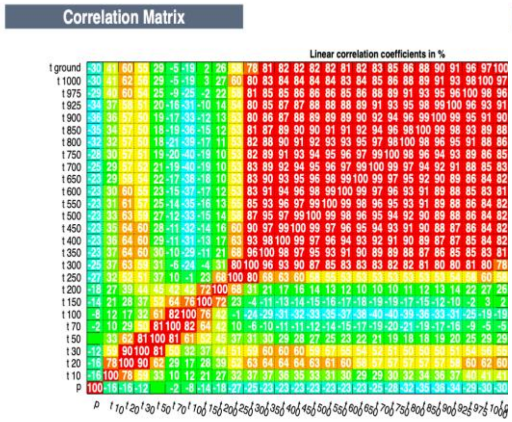

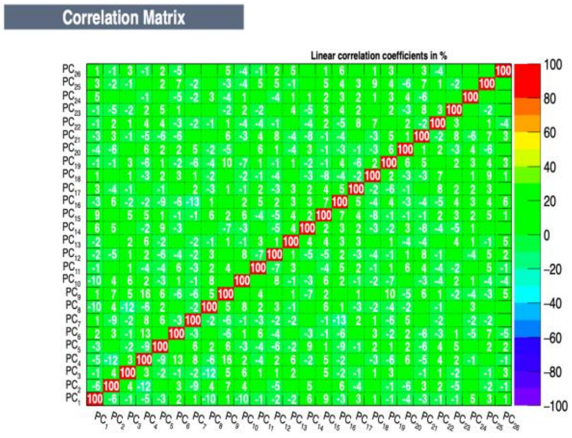

Muons and temperature of the atmosphere

- Also this procedure is reducing dimensionality of the problem by choosing only statistically meaningful.
- Method is more efficient then others but our alternative method which use machine learning is even more efficient.

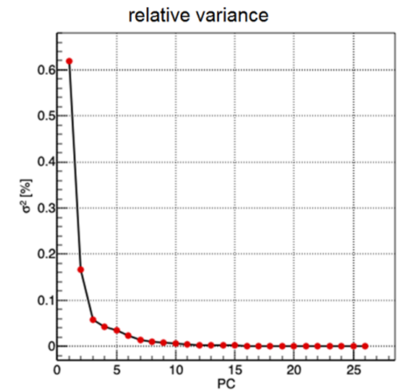

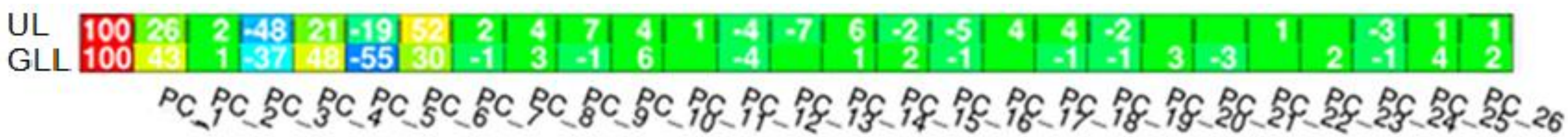

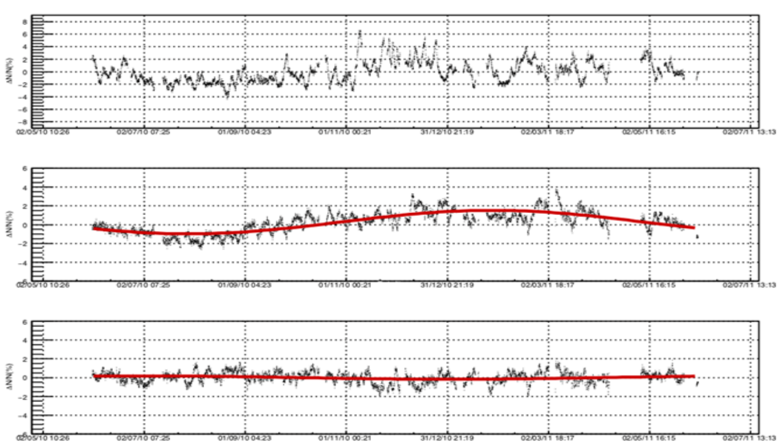
64.5% variance reduction

GLL

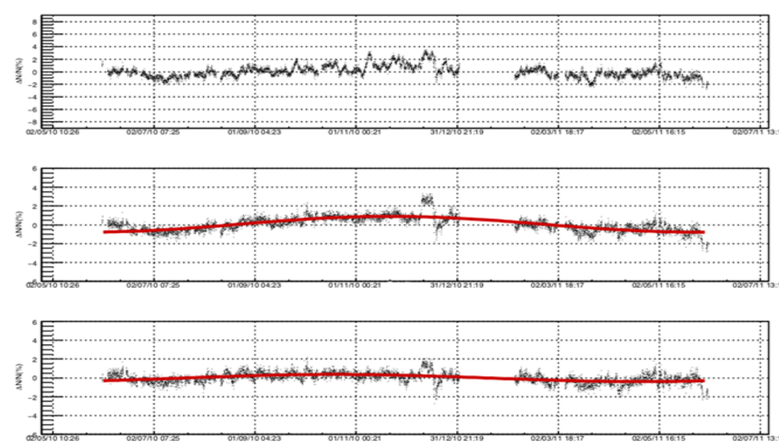
38.1% variance reduction

UL

Muons and temperature of the atmosphere

- The effect of atmospheric parameters in secondary cosmic ray muon component is well known. There are several theoretical and empirical models that describe these effects well. Usually this knowledge is used to correct for secondary cosmic ray variations due to atmospheric effects.
- Alternatively, once model parameters are established, sensitivity of cosmic ray muon detectors to variations od atmospheric origin can be used to estimate temperatures for different layers of the atmosphere.
- We demonstrate this procedure using cosmic ray data measured in our lab, combined with parameters of our empirical model for meteorological effects based on principal component analysis.

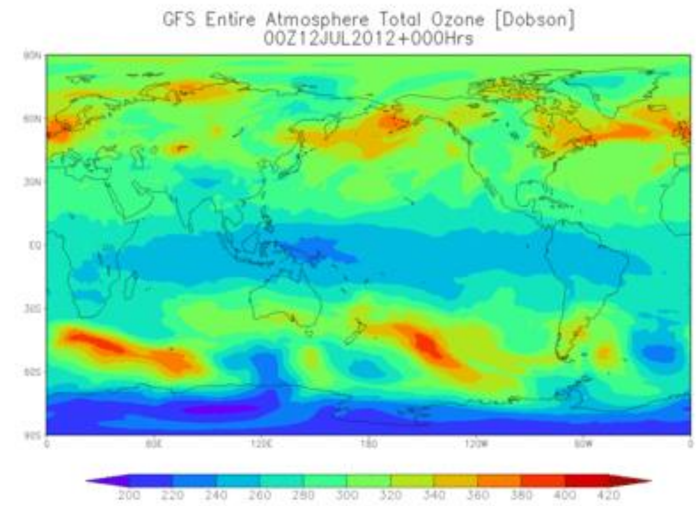

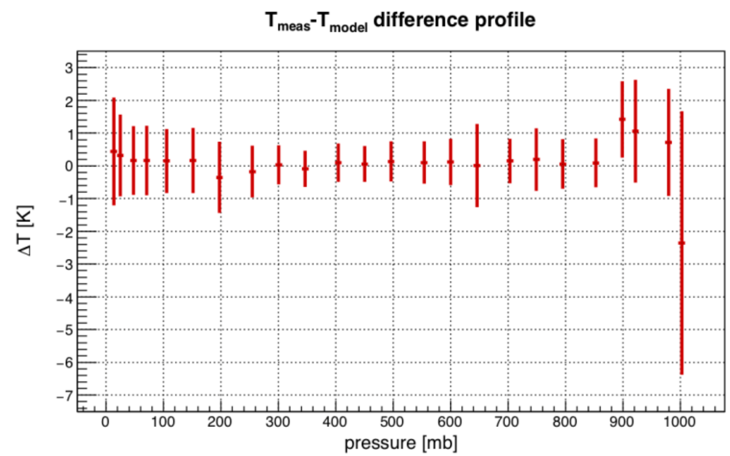

Muons and temperature of the atmosphere

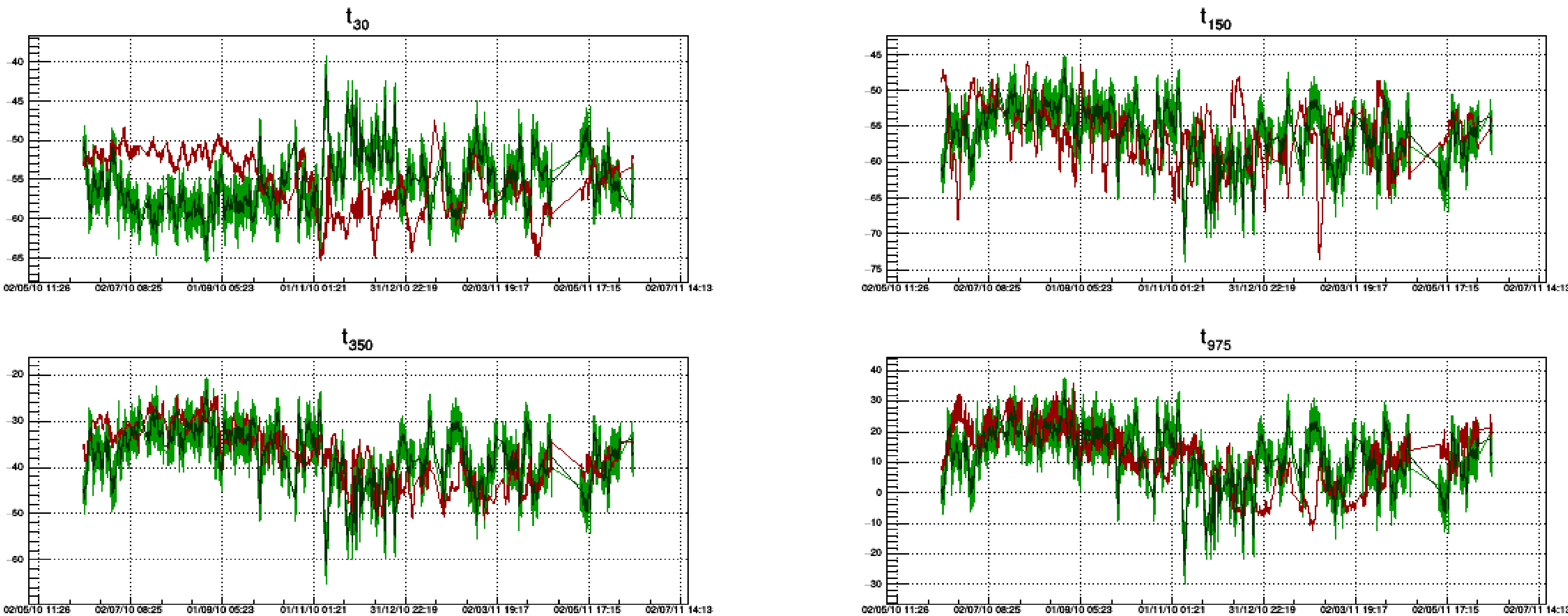

Time series of measured (red) and estimated temperature (green and dark green) for isobaric levels 30, 150, 350 i 975 mbar. Preliminary data!

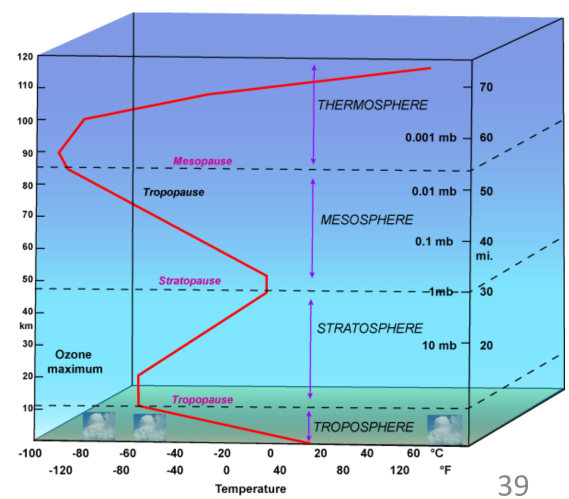

Cloudiness and cosmic rays

- The physical mechanism proposed to explain CR contribution to cloud formation is named ion-induced nucleation
- Diurnal temperature range (DTR) is the difference between daily temperature maximum and minimum DTR = Tmax − Tmin .It is a useful quantity since it is anticorrelated with cloudiness is used as a proxy for cloudiness.
- An index of DTR deviations is defined combining temperature data from multitude of north hemisphere meteorological stations. This is the excursion od DTR from the expected value, and this difference, normalized to standard deviation.
- DTR deviation index time series are studied, searching for variations correlated with CR variations, with the aim of testing the hypothesis of CR influence on cloud cover
- Superposed epoch analysis on the set of Forbush decreases above certain amplitude cut has been performed.
- When the cut is raised to 7%, the DTR deviations start to differ significantly from zero in the days following FD.

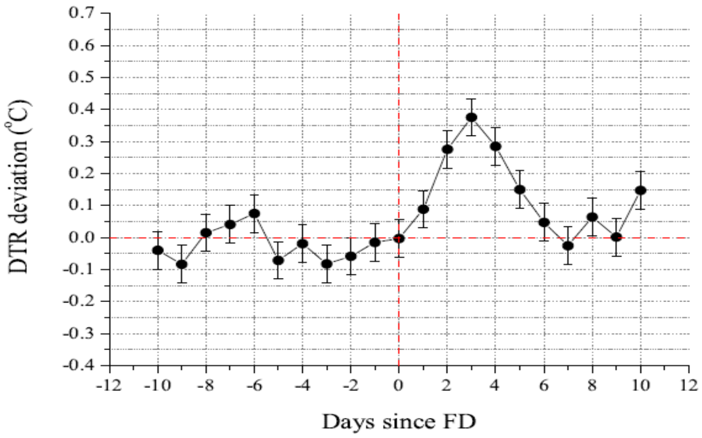

Fig. 3. Superposed epoch analysis of DTR deviation before and during Forbush decrease with amplitude higher than 7% (35 FD events). Zero epoch is the day of the FD start. The error bars represent the standard error of the mean.

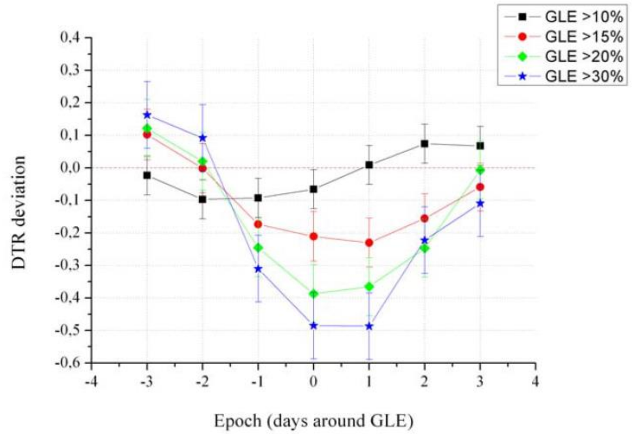

Average deviations of DTR values from their expected average values for the days around the appearance of the GLE effects, for different GLE amplitudes.

Cloudiness and cosmic rays

- The physical mechanism proposed to explain CR contribution to cloud formation is named ion-induced nucleat
- Diurnal tempera between daily te minimum DTR = quantity since it used as a proxy
- An index of DTI temperature dat hemisphere met excursion od DT this difference, r
- DTR deviation ir searching for va variations, with t CR influence on
- Superposed epc decreases abov performed.
- When the cut is raised to 7%, the DTR deviations start to differ significantly from zero in the days following FD.

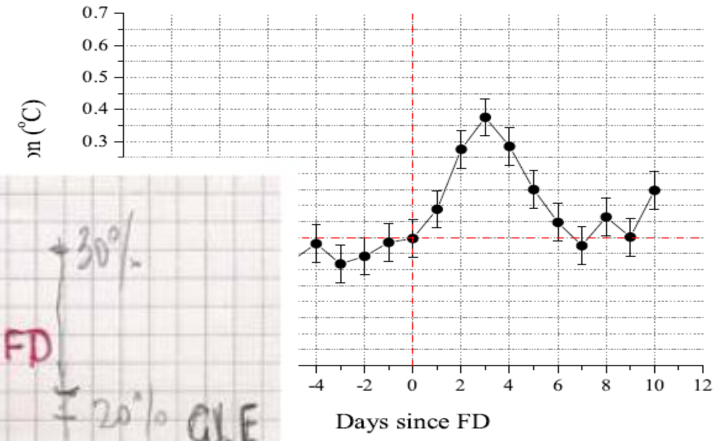

analysis of DTR deviation before and
ith amplitude higher than 7% (35 FD
ay of the FD start. The error bars repre-
e mean.

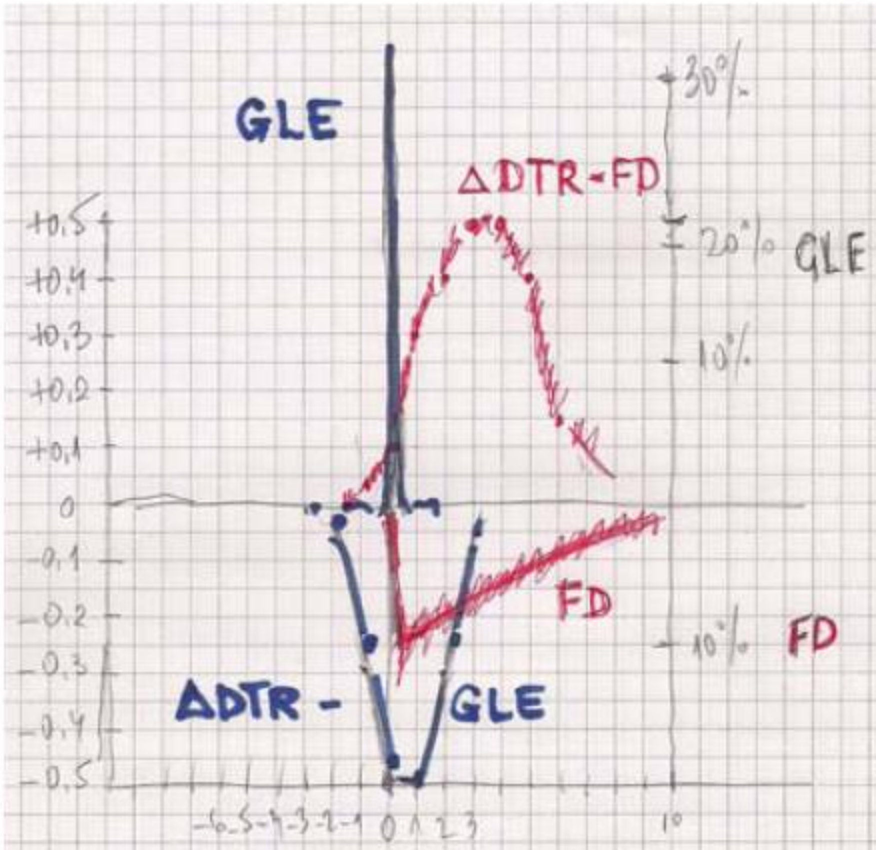

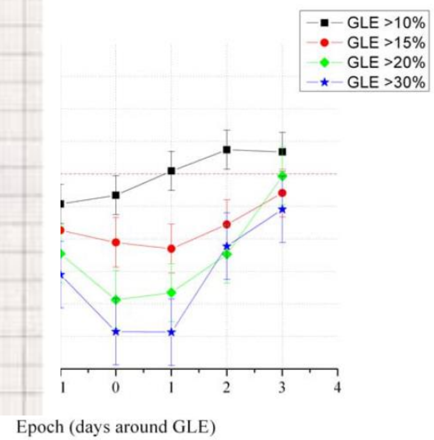

Average deviations of DTR values from their expected average values for the days around the appearance of the GLE effects, for different GLE amplitudes.

Arduino detector

- Based on MIT project for hendheld muon detector-Cosmic watch
- With collaboration with one highschool (for gifted children)
- Telescope arrangement of two plastic scintilators with MPPS/SiPM

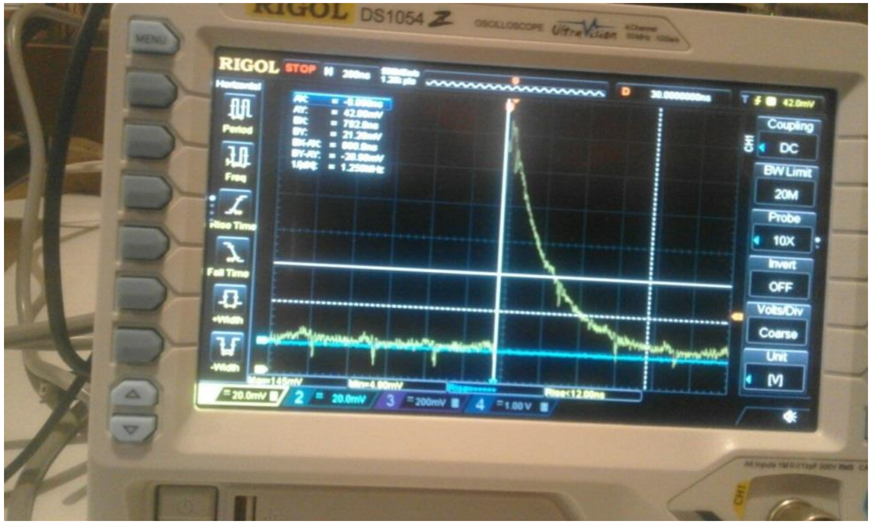

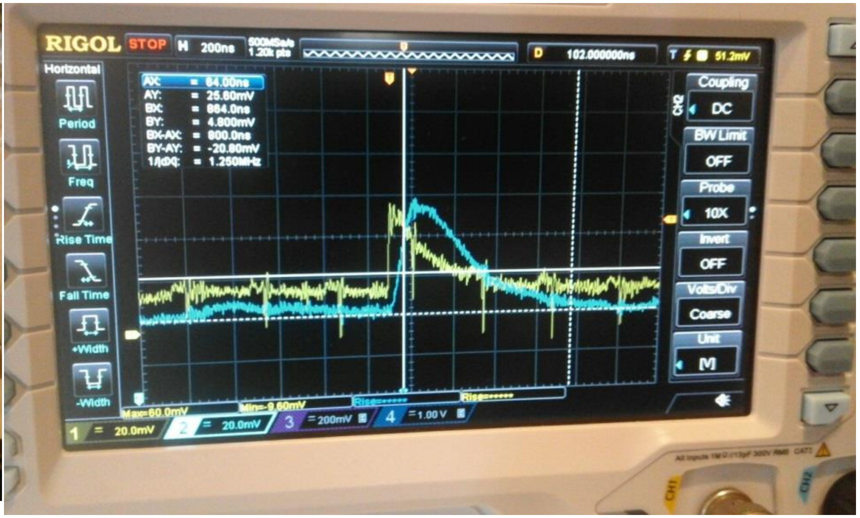

Need improvement!

Plans for future

- Exploring correlation of the CR with enviromental parameters measured at the site (atmospheric parameters, soil composition, particles in air, cloudiness,...)
- CR induced radiation (cosmogenic radionuclides) in the enviroment (past and present) and in the detectors (active shielding, understanding background noise)
- New CR detectors and outreach
- Organizing an international workshop on radiation and enviroment next year

Conclusion

- Muon detectors at Low level laboratory are used to find rigidity dependence of Forbush decrease. These data for transient solar modulation of GCR are obtained over much higher range of rigidities than region sensitive to NM thus allowing more extensive studies of cosmic-ray solar modulation processes.

- Comparison of ground data with satellite data outside geomagnetic field shows different correlation depending on energy recorded particles thus allowing better understanding of correlation between Forbush decreases and CME that can lead to hazardous event on Earth.

- Dependence of FD amplitude on median rigidity can lead to better models of propagation of CR through heliosphere thus giving condition of the heliosphere.
- Small detectors can be used to monitor not just solar weather but also some CR induced effects in enviroment

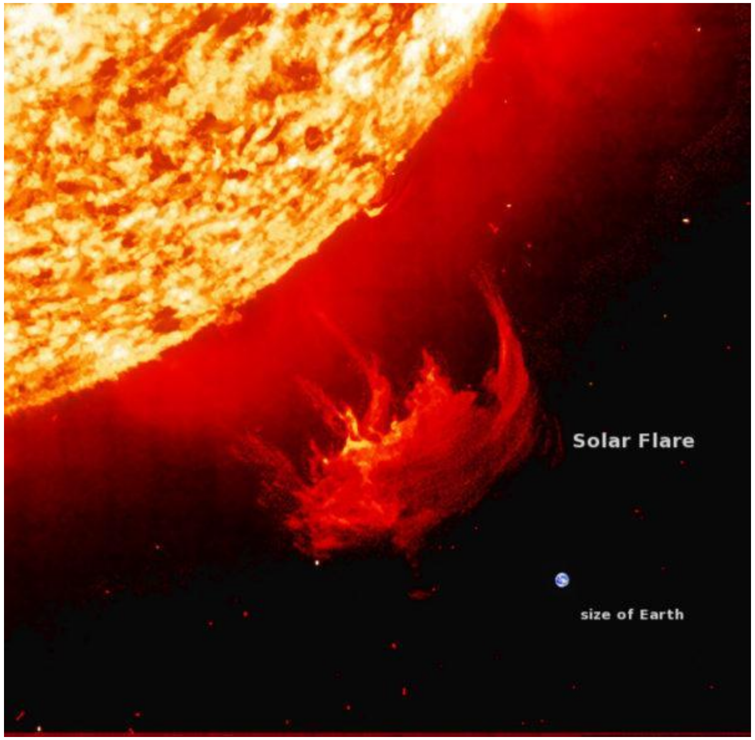

Thank you for your attention!

http://cosmic.ipb.ac.rs/

Backside slides

Low-background laboratory for nuclear physics

Past activities

- Plasma focus device
  - The plasma focus experiment in Belgrade, Serbia started in the late eighties of the last century. Belgrade plasma focus device (BPFD) is a fusion machine intended to operate as optimized neutron source or hard X-ray source and can be used for neutron activation or production of short-living radioisotopes. These radioisotopes will have very low activity which can be analyzed in the underground Low-Background Laboratory for Nuclear Physics. Also, we compared the obtained experimental data (neutron yield, total current waveform, working gas pressure) with the numerical simulation code (The Lee model code) to test our plasma focus machine. Comparison between neutron yield from our experimental data and neutron scaling laws and neutron yields derived from computation using the Lee Model code shows good matching, but for better verification of the code, more experimental data are needed.

Capacity (μF)	45
Voltage (kV)	15
Inductivity (nH)	62
Peak current (kA)	300
Energy input (kJ)	5
Anode diameter (cm)	0.95
Pressure (mbar)	3.5
Averaged neutron yield (neutron3/pulse)	2 x 10^7
Distance between outer and inner electrode (cm)	3
Length of the inner electrode (cm)	19

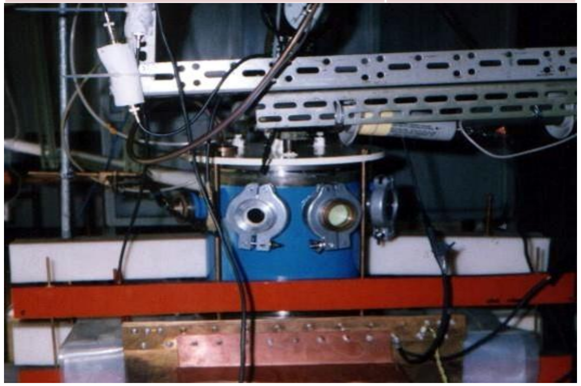

Експерименталне поставке

- First one was to extend the sensitivity to 94 higher energies with detection of multi-muon events underground. An array of horizontally oriented muon detectors ought to be placed in the UL. Simultaneous triggering of more than one detector is an indication of a multi-muon event.
- The idea was exploited in the EMMA underground array located at the deeper underground laboratory in Pyhasalmi mine, Finland, with the intention to reach energies in the so called knee region.
- For a shallow underground laboratory, exceeding the energy region of solar modulation would open the possibility to study CR flux variations originating outside of the heliosphere.
- На основу симулације број мултимионских догађаја је сувише мали да би се само уз помоћ садашње опреме могле пратити промене флукса услед соларних модулација која је реда неколико процената дневно. Да би се детектовале промене флукса реда 1% са 3σ извесношћу ($3\sqrt{N}/N$), потребно је проширити детекторски систем да би добили потребан интензитет флукса. Уколико се систем за детекцију миона прошири на целу површину подземног дела Нискофонске лабораторије (слика 5.24). Из симулације се добија ~2600 коинциденција по дану, детектованих у по два детектора (површине 1m^2), на различитим могућим растојањима на целој површини. Овај број омогућава, са потребном статистичком сигурношћу, посматрање варијација већих од 5,8% које потичу од соларне модулације. Овакве варијације флукса се ретко јављају (нпр. веома велико Форбушово смањење) па је ова поставка неодговарајућа за континуално посматрање флукса на различитим енергијама примарног космичког зрачења
- Важно је и да се узимају у обзир само коинциденције настале од миона а не и од електромагнетне компоненте. Електромагнетна компонента (δ електрони, фотони и слично) настаје у интеракцији миона са земљиштем изнад детектора. Овакав „мини пљусак“ је локализован око миона, а те честице се могу детектовати у детектору и погрешно идентификовати као мионi. Да би се избегла оваква лажна коинциденција потребно је коинцидирати догађаје са већих растојања

Detektorski sistemi

Funkcija odziva (Response function)

- **Odbroj detektora** se može prikazati sa:

$$N_d = \sum_i \int_{E_{th}}^{\infty} Y_i\,(E,h) \cdot J_i(E,t)dE = \int_{E_{th}}^{\infty} W_t\,(E,h,t)dE$$

- Funkcija $J_i(E,t)$ je spektar energija primarnog kosmičkog zračenja
- $Y_i(E,h)$ je funkcija prinosa za datu energiju i visinu.

$$Y_i(E,h) = \int_{E_{th}}^{\infty} \int S_i\,(\theta,\phi) \cdot \Phi_{i,\mu}(E_i,h,E,\theta,\phi)dEd\Omega$$

$S_i(\theta,\phi)$ efektivna površina detektora

$\Phi_{i,\mu}(E_i,h,E,\theta,\phi)$ je diferencijalni fluks miona po primarnoj čestici *i* tipa sa energijom E_i.

$W_t\,(E,h,t)$ je diferencijalna **funkcija odziva**

- Metod parametrizacije, teorijski metod ili uz pomoć simulacije se određuje https://soho.nascom.nasa.gov/classroom/nordlys_english.mov

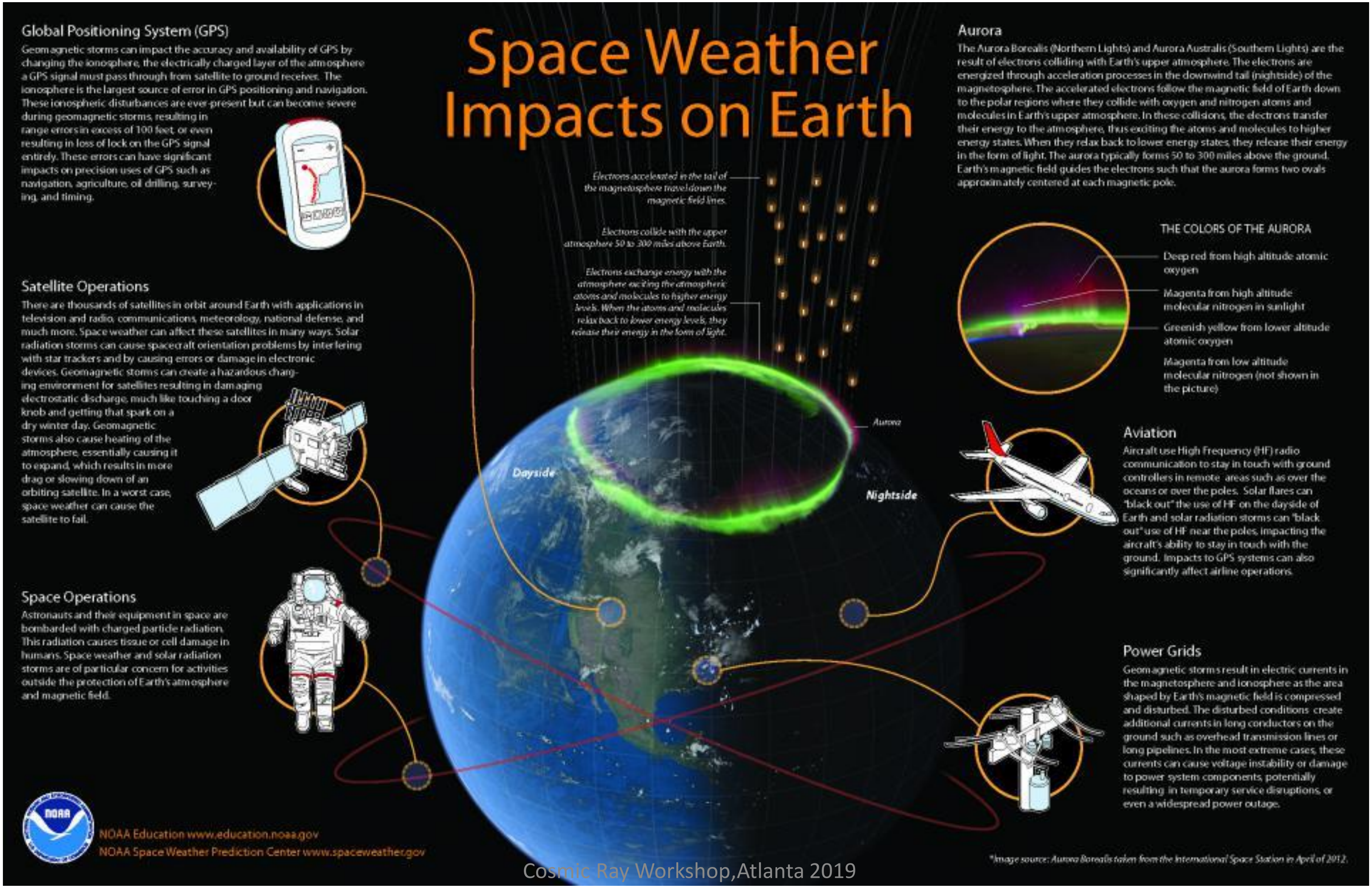

Симулациони пакети CORSIKA и GEANT4

- Коришћено 10^9 примарних протона и алфа честица приликом симулирања атмосферске каскаде

RUNNR	20907	Број симулације
EVTNR	1	Редни број прве честице
NSHOW	1000000	Укупан број примарних честица
PRMPAR	14	Тип примарне честице, у овом примеру протон
ESLOPE	-2.7	Експоненцијални коефицијент енергије
ERANGE	1 2.E7	Интервал енергија примарних честица у GeV-а
THETAP	0. 70.	Распон зенитних углова упадне примарне честице у степенима
PHIP	-180. 180.	Распон азимутних углова упадне примарне честице у степенима
SEED	814 0 0	seed за прву секвенцу случајних бројева
SEED	1114 0 0	seed за другу секвенцу случајних бројева
OBSLEV	7.80E+03	Опсервациони ниво (у cm)
FIXCHI	0	Почетна висина (g/cm^2)
MAGNET	22.7 42.1	Геомагнетно поље за Београд
ATMOD	4	Атмосферски профил дат са 5 нивоа. Овде профил ATM511 изнад Штудгарта измереног маја 1993. године
QGSJET	T 0	Укључена QGSJET01c рутина за симулацију високоенергетских хадрон-нуклеус и нуклеус-нуклеус судара
ECUTS	0.15 0.15 0.0015 0.0015	Доњи праг енергија (у GeV) за честице које се прате и то за хадроне, мионе, електроне и фотоне
MUADDI	T	Додатни подаци о месту и начину креације миона се такође прате

Простирање космичког зрачења кроз земљиште

- Миони при проласку кроз земљиште производе терцијалне каскаде

- Мион губи енергију при кретању двојако, континуално и дискретно.
  - Континуално губи енергију кроз јонизацију
  - Дискретни губици енергије продукцију електрон-позитрон парова, закочно зрачење и електромагнетна интеракција са језгром.

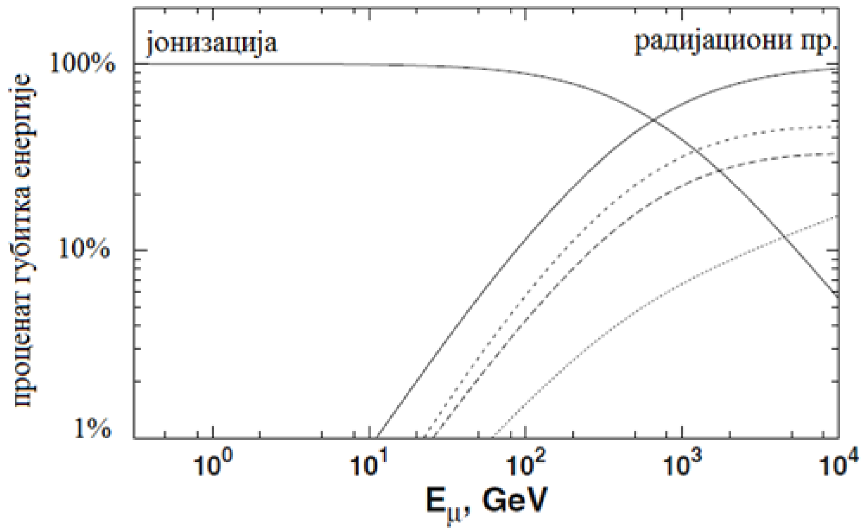

Измерени подаци – флукс миона

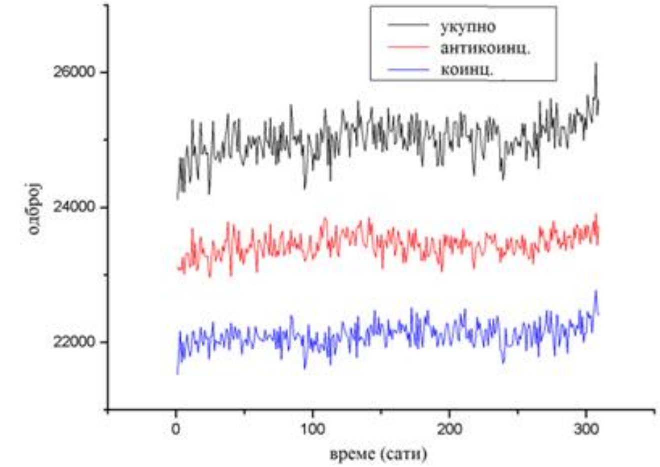

- Увођење нове опреме у лабораторију се поклапа са почетком 24. Соларног циклуса

Φ=46,53 $m^{-2}s^{-1}$

- Флукс миона за подземни део

Φ_{cc}=24.89 $m^{-2}s^{-1}$ и Φ_{anti}=21.64 $m^{-2}s^{-1}$.

$$\Phi = \frac{N}{S \cdot \varepsilon \cdot t}$$

- Декохеренција

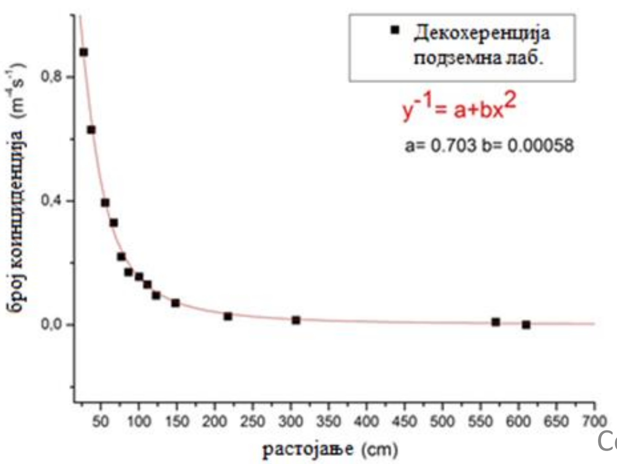

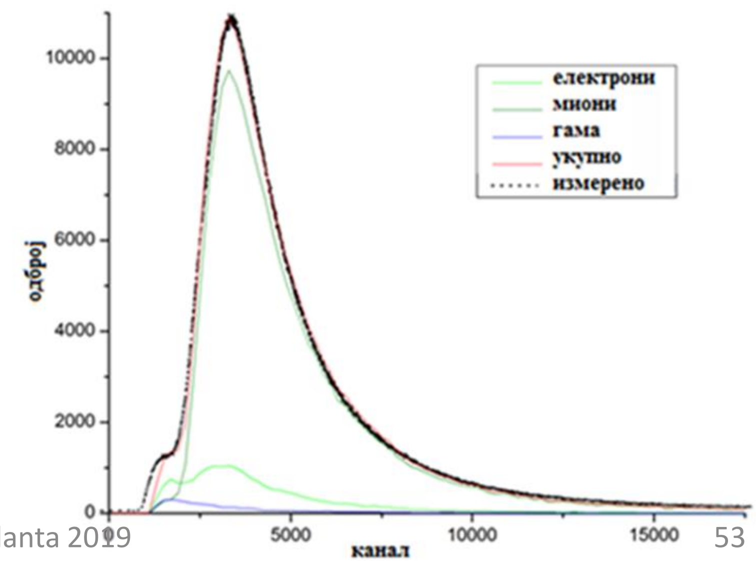

Detektorski sistemi

Poređenja

- Poređenje sa bliskim Neutronskim detektorima
- Utvrđen je stepen linearne korelacije

$$r = r_{xy} = \frac{\sum_{i=1}^{n}(x_i - \bar{x})(y_i - \bar{y})}{\sqrt{\sum_{i=1}^{n}(x_i - \bar{x})^2}\sqrt{\sum_{i=1}^{n}(y_i - \bar{y})^2}}$$